The Plant Cell, Vol. 21: 2485–2502, August 2009, www.plantcell.org

Control of Nuclear and Nucleolar Localization of Nuclear Inclusion Protein a of Picorna-Like *Potato virus A* in *Nicotiana* Species [W]

Minna-Liisa Rajamäki[1] and Jari P.T. Valkonen

Department of Applied Biology, University of Helsinki, Helsinki FIN-00014, Finland

The multifunctional nuclear inclusion protein a (NIa) of potyviruses (genus *Potyvirus*; Potyviridae) accumulates in the nucleus of virus-infected cells for unknown reasons. In this study, two regions in the viral genome-linked protein (VPg) domain of NIa in *Potato virus A* (PVA) were found to constitute nuclear and nucleolar localization signals (NLS) in plant cells (*Nicotiana* spp). Amino acid substitutions in both NLS I (residues 4 to 9) and NLS II (residues 41 to 50) prevented nuclear localization, whereas mutations in either single NLS did not. Mutations in either NLS, however, prevented nucleolar localization and prevented or diminished virus replication in protoplasts, accumulation in infected plant tissues, and/or systemic movement in plants. One NLS mutant was partially complemented by the wild-type VPg expressed in transgenic plants. Furthermore, NLS I controlled NIa accumulation in Cajal bodies. The VPg domain interacted with fibrillarin, a nucleolar protein, and depletion of fibrillarin reduced PVA accumulation. Overexpression of VPg in leaf tissues interfered with cosuppression of gene expression (i.e., RNA silencing), whereas NLS I and NLS II mutants, which exhibited reduced nuclear and nucleolar localization, showed no such activity. These results demonstrate that some of the most essential viral functions required for completion of the infection cycle are tightly linked to regulation of the NIa nuclear and nucleolar localization.

INTRODUCTION

It is largely unknown why proteins encoded by positive-strand RNA viruses that replicate in membranous structures in the cytoplasm are localized in the nucleus (Salonen et al., 2004; Miller and Krijinse-Locker, 2008). There are indications that these viruses target the nucleus to recruit or sequester certain nuclear components or suppress host defense (Hiscox, 2003, 2007). For example, infection with animal viruses can induce changes in the nucleocytoplasmic distribution of host proteins (Hiscox, 2003). The 2b protein of *Cucumber mosaic virus*, a single-stranded RNA virus (genus *Cucumovirus*, family Bromoviridae), localizes to the nucleus and suppresses RNA silencing, a fundamental antiviral mechanism in plants (Lucy et al., 2000). By contrast, translocation of the P19 protein of *Tomato bushy stunt virus* (genus *Tombusviru*s, family Tombusviridae) to the nucleus by plant ALY proteins appears to downregulate the suppressor activity of P19 (Canto et al., 2006). A few viral proteins are also found in the nucleolus. The nucleolus is involved in rRNA synthesis, ribosome biogenesis, cell cycle regulation, stress responses, and gene silencing (Olson et al., 2000; Pontes et al., 2006; Boisvert et al., 2007). Viral proteins in the nucleolus either redistribute nucleolar proteins to alter nucleolar functions or recruit nucleolar proteins to facilitate viral replication (Hiscox, 2007). In plant cells infected with *Groundnut rosette virus* (GRV; genus *Umbravirus*), the GRV ORF3 protein enters the nucleus and accumulates in the nucleolus and Cajal bodies (CBs), small subnuclear bodies, or structures (Ryabov et al., 2004; Kim et al., 2007b). This viral protein interacts with the nucleolar protein fibrillarin, which is required for long-distance viral movement in plants (Kim et al., 2007a, 2007b; Canetta et al., 2008).

Potyviruses (genus *Potyvirus*, family Potyviridae) constitute the largest group of plant-infecting RNA viruses (Rajamäki et al., 2004). They belong to the picorna-like supergroup of positive-sense single-stranded RNA viruses (Goldbach, 1986) and encode a large polyprotein that is subsequently cleaved by three virus-encoded proteinases to yield up to 10 mature proteins (Rajamäki et al., 2004) (Figure 1). Additionally, a 6- to 7-kD protein is produced from the P3 protein–coding region by frameshifting (Chung et al., 2008). Nuclear inclusion protein b (NIb; replicase) and the main viral proteinase, NIa, localize to the nucleus where they may induce nuclear inclusions (Knuhtsen et al., 1974; Dougherty and Hiebert, 1980; Edwardson and Christie, 1983; Restrepo et al., 1990; Martin et al., 1992; Hajimorad et al., 1996). Furthermore, NIa proteins of *Tobacco etch virus* (TEV) and *Turnip mosaic virus* have been detected in the nucleolus (Restrepo et al., 1990; Beauchemin et al., 2007). NIa is processed in cis at an internal suboptimal proteolytic cleavage site by the C-proximal proteinase domain (NIa-Pro) (Carrington and Dougherty, 1987). In infected cells, the majority of NIa accumulates (as the unprocessed form) in the nucleus (Carrington et al., 1993). In the nucleus, *Turnip mosaic virus* NIa interacts with the translation initiation factor eIF(iso)4E and the poly(A) binding protein (Beauchemin et al., 2007; Beauchemin and Laliberté, 2007).

[1] Address correspondence to minna.rajamaki@helsinki.fi.
The author responsible for distribution of materials integral to the findings presented in this article in accordance with the policy described in the Instructions for Authors (www.plantcell.org) is: Minna-Liisa Rajamäki (minna.rajamaki@helsinki.fi).
[W] Online version contains Web-only data.
www.plantcell.org/cgi/doi/10.1105/tpc.108.064147

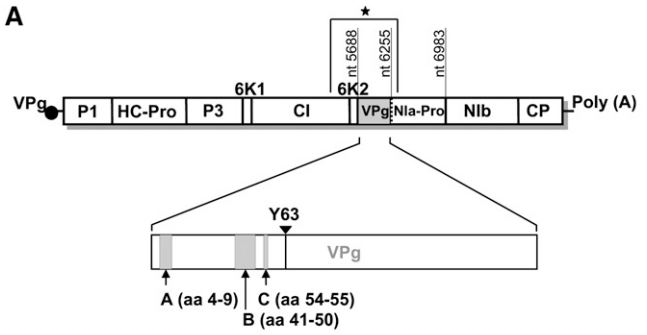

icPVA	Recombinant construct			Amino acid sequences in putative NLS regions A (aa 4-9)	B (aa 41-50)	C (aa 54-55)
wtPVA	VPgN	VPg	NIa	KRQRQK	KKGKTKGKTHGMGKK	
PVA-a	VPgN(a)	VPg(a)	NIa(a)	**A**A**A**Q**A**Q**A**	KKGKTKGK THGMGKK	
-	VPgN(ab)	-	-	**A**A**A**Q**A**Q**A**	**A**A**A**G**A**T**A**G**A**THGMGKK	
-	VPgN(b)	VPg(b)	NIa(b)	KRQRQK	**A**A**A**G**A**T**A**G**A**THGMGKK	
-	VPgN(bc)	-	-	KRQRQK	**A**A**A**G**A**T**A**G**A**THGMG**A**A	
-	VPgN(abc)	-	-	**A**A**A**Q**A**Q**A**	**A**A**A**G**A**T**A**G**A**THGMG**A**A	
PVA-b1	b1N	VPg-b1	NIa(b1)	KRQRQK	K**A**G**A**TKGK THGMGKK	
PVA-b2	b2N	VPg-b2	NIa(b2)	KRQRQK	K**A**GK**A**KGK THGMGKK	
PVA-b3	b3N	VPg-b3	NIa(b3)	KRQRQK	K**A**G**A**A**A**KGK THGMGKK	
PVA-b4	b4N	VPg-b4	NIa(b4)	KRQRQK	KKG**A**A**A**KGK THGMGKK	

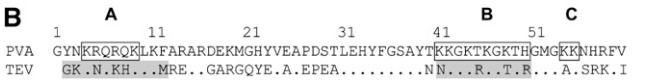

Figure 1. Putative NLS in the VPg Domain of the NIa Protein.

(A) Schematic presentation of the genome and cistrons corresponding to mature proteins in PVA: P1, proteinase; HC-Pro, helper component-proteinase; P3, the third protein; 6K1 and 6K2, 6-kD proteins 1 and 2; CI, helicase; NIa-Pro, proteinase; NIb, replicase; and CP, coat protein (Rajamäki et al., 2004). The VPg region is magnified to show details. A, B, and C denote putative NLS domains. Residue Tyr-63 in the PVA VPg is presumably responsible for linking VPg covalently the 5′ terminus of viral RNA (Germundsson et al., 2007). The region marked with star is flanked by unique *Swa*I and *Apa*I sites in the infectious cDNA of PVA (icPVA) and was used for site-directed mutagenesis. The genomic positions (nucleotides) of the NIa coding region and the internal proteolytic site for separation of VPg and NIa-Pro (a dashed line) are indicated. The table shows residues of the wild-type and mutated VPg domains introduced into the infectious cDNA of PVA or used in transient expression constructs. The names ending with N indicate that the 55 N-proximal residues of VPg are fused to two marker proteins (e.g., VPgN-GUS-GFP). For brevity, the GUS-GFP marker proteins are not included in construct names. Constructs named as NIa are fused to the C terminus of GFP (GFP-NIa). Mutated residues are in bold and underlined. aa, amino acids.
(B) Alignment of the N-proximal residues in the VPg of PVA and TEV. Numbering is according to PVA. Only the amino acid residues that differ from those of PVA are shown. Putative NLS domains A, B, and C in PVA VPg are boxed, whereas the two regions implicated in nuclear localization of TEV NIa are shaded (Carrington et al., 1991; Schaad et al., 1996).

NIa is a multifunctional protein; thus, the ramifications of its nuclear and nucleolar localization are of particular interest. The NIa-Pro domain has sequence-nonspecific DNase activity and proteinase activity (Carrington and Dougherty, 1987; Anindya and Savithri, 2004), whereas all other known functions of NIa are regulated by the viral genome-linked protein (VPg) constituting the N-proximal domain. VPg has NTP binding activity, is uridylylated by the viral RNA polymerase (NIb), and may act as a primer for synthesis of viral RNA (Murphy et al., 1996; Schaad et al., 1996; Puustinen and Mäkinen, 2004; Anindya et al., 2005). VPg is covalently linked to the 5′-end of the viral genomic RNA via a conserved Tyr (residue 60) in *Tobacco vein mottling virus* (Murphy et al., 1991), which in *Potato virus A* (PVA) corresponds to residue 63. Substitution of this Tyr residue with other amino acids abolishes infectivity of both viruses (Murphy et al., 1996; Germundsson et al., 2007). The intrinsically disordered structure of VPg (Grzela et al., 2008; Rantalainen et al., 2008) provides flexibility for many types of interactions with viral and host proteins (Hong et al., 1995; Li et al., 1997; Wittmann et al., 1997; Schaad et al., 2000; Guo et al., 2001; Dunoyer et al., 2004; Léonard et al., 2004; Thivierge et al., 2008). Interactions between eIF4E or eIF(iso)4E (Wittmann et al., 1997; Schaad et al., 2000; Robaglia and Caranta, 2006) and VPg or NIa are important for virus infectivity (Léonard et al., 2000; Robaglia and Caranta, 2006). VPg is also involved in viral cell-to-cell and long-distance movement (Nicolas et al., 1997; Schaad et al., 1997; Rajamäki and Valkonen, 1999, 2002, 2004).

The control of NIa nuclear localization has been studied in TEV (Carrington et al., 1991; Schaad et al., 1996). The TEV NIa nuclear localization signal (NLS) is located at the N-proximal part of the VPg. Initially, it was thought to consist of two regions defined by residues 1 to 11 and 43 to 72, both of which are required for efficient nuclear localization of a β-glucuronidase/NIa (GUS-NIa) fusion protein (Carrington et al., 1991). However, further studies showed that residues 40 to 49 constitute the NLS, whereas the N-terminal residues contribute to optimal nuclear translocation of NIa (Carrington et al., 1991; Schaad et al., 1996). Substitution of residues K41, K43, R44, and T48 in VPg reduce NIa nuclear localization and TEV infectivity (Schaad et al., 1996), indicating that NIa nuclear localization may be important for potyvirus infection.

The aim of this study was to investigate further the regulatory mechanisms of nuclear and nucleolar localization of NIa and to establish whether NIa localization is important for infection of plants. Two regions at the N-proximal part of the VPg in PVA were found to control both nuclear and nucleolar localization of marker fusion proteins. One of these regions also controlled protein localization to CBs. Mutations in the NLS regions of VPg reduced PVA infectivity in protoplasts and plants. Overexpression of VPg complemented a noninfectious mutant of PVA and delayed gene silencing (cosuppression) in transgenic plants. These results demonstrate that some of the most essential viral functions required for completion of the infection cycle are tightly linked to the control of NIa nuclear and nucleolar localization.

RESULTS

Nuclear Localization of PVA NIa and VPg

The majority of NIa is detected in the nucleus of PVA-infected cells in systemically infected leaves of *Solanum commersonii* (Rajamäki and Valkonen, 2003) and tobacco (*Nicotiana tabacum*) (Figure 2A), as determined by immunostaining with antibodies

against VPg and NIa-Pro. To examine whether NIa and VPg are targeted to the nucleus in the absence of PVA infection, the proteins were expressed as fusions to the C terminus of green fluorescent protein (GFP-NIa and GFP-VPg) (Figure 3) in leaves of *Nicotiana benthamiana* by agroinfiltration. To prevent the cleavage between VPg and NIa-Pro domains and to study localization of unprocessed NIa, the P1 position of the internal cleavage site was mutagenized [substitution E189H; construct GFP-NIa(E/H); see Supplemental Figure 1A online]. Fluorescence microscopy revealed that GFP-NIa, GFP-NIa(E/H), and GFP-VPg accumulated predominantly in the nucleus, with little or no fluorescence observed in the cytoplasm (Figure 2C; see Supplemental Figure 1B online). By contrast, GFP alone localized to both the cytoplasm and nucleus (Figure 2B).

Regions of the VPg Domain Controlling Nuclear Localization

Residues 41 to 50 (KKGKTKGKTH) form the putative NLS of PVA NIa, based on comparison with the TEV NIa NLS (Figure 1B) (Schaad et al., 1996). Therefore, the full-length VPg domain of PVA NIa, the N-terminal part of VPg (VPgN; residues 1 to 55), the putative NLS (residues 41 to 50) within the VPg domain, and the NLS of TEV VPg (residues 40 to 49) were each expressed as a fusion with GUS-GFP (Figure 3). The large GUS-GFP fusion protein was used to prevent spontaneous movement of GFP to the nucleus (Grebenok et al., 1997). The constructs were introduced for expression in the epidermal cells of *N. benthamiana* leaves by particle bombardment and/or agroinfiltration. VPgN-GUS-GFP was detected almost exclusively in the nucleus, whereas GUS-GFP was localized in the cytoplasm (Figure 4), showing that the N-terminal 55 residues of VPg were sufficient to target GUS-GFP to the nucleus and hence contained the NLS of PVA NIa. By contrast, the majority of VPg-GUS-GFP, PVAnls-GUS-GFP, and TEVnls-GUS-GFP were detected in the cytoplasm (see Supplemental Figure 2 online). In PVAnls-GUS-GFP and TEVnls-GUS-GFP, the residues constituting an NLS may have been masked by the putative conformation of the large GUS-GFP protein, which may have prevented nuclear localization. Constructs based on VPgN-GUS-GFP and GFP-NIa were thus used for further analysis.

The four residues critical for nuclear localization of TEV NIa are Lys-41, Lys-43, Arg-44, and Thr-48 (Schaad et al., 1996). They correspond to Lys-42, Lys-44, Thr-45, and Thr-49, respectively, in PVA NIa and define the putative NLS region designated as B (Figure 1). In TEV, substitution of two or three of the residues Lys-41, Lys-43, or Arg-44 with Ala perturbs nuclear transport of NIa, whereas substitution of single residues has little effect (Schaad et al., 1996). When two or three of the corresponding residues of the putative NLS region B in PVA NIa were substituted with Ala in GFP-NIa and VPgN-GUS-GFP (mutations b1N, b2N, b3N, and b4N; Figure 1), all mutant proteins showed similarly reduced nuclear localization compared with VPgN-GUS-GFP (Figures 4A and 4C to 4F) and GFP-NIa (see Supplemental Figure 1B online). Because the region B in PVA contains three Lys residues in

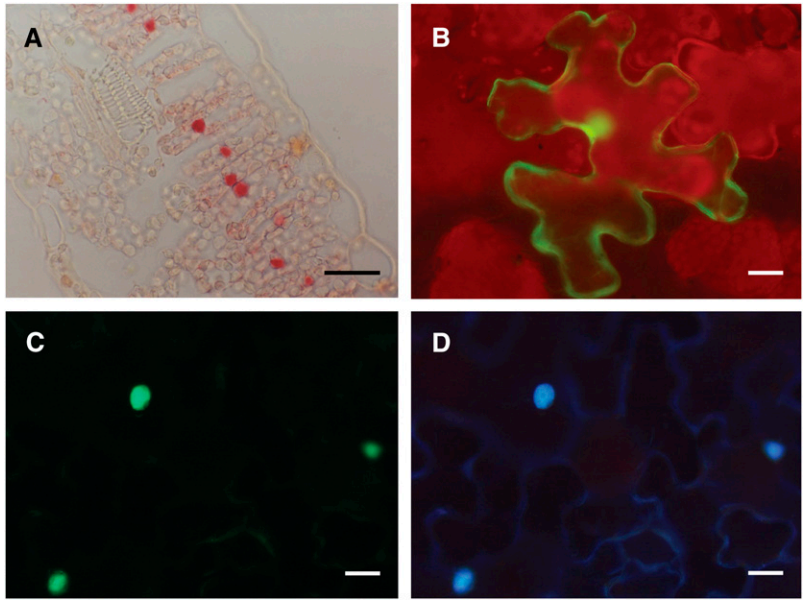

Figure 2. Nuclear Localization of NIa of PVA in Cells of *N. tabacum* and *N. benthamiana*.

(A) Immunohistochemical localization with antibodies against VPg in upper noninoculated leaves of *N. tabacum* systemically infected with PVA at 20 DAI as described (Rajamäki and Valkonen, 2003). Immunostaining signals (red) were detected mainly in the nucleus.
(B) Localization of GFP (not fused to NIa) in the cytoplasm and nucleus of epidermal cells of an agroinfiltrated leaf of *N. benthamiana* 3 DAIF.
(C) GFP-NIa transiently expressed by agroinfiltration and detected by epifluorescence microscopy 3 DAIF.
(D) The 4',6-diamidino-2-phenylindole (DAPI) staining indicates the positions of nuclei in cells shown in **(C)**. Red autofluorescence caused by chlorophyll is visible in **(B)** due to filter settings that differ from those in **(C)**. Bars = 25 μm.

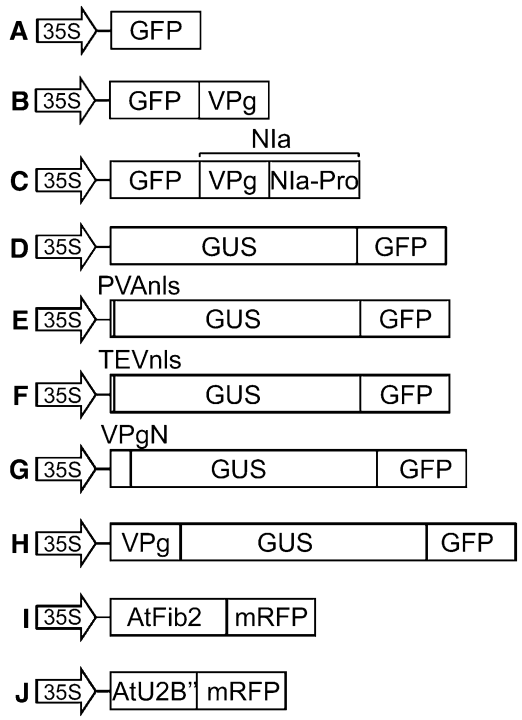

Figure 3. Schematic Presentation of the Constructs Used for Protein Expression and Localization Studies.

(A) pRT-GFP, **(B)** pRT-GFP-VPg, **(C)** pRT-GFP-NIa, **(D)** pRT-GUS-GFP, **(E)** pRT-PVAnIs-GUS-GFP (PVAnIs refers to region B in Figure 1), **(F)** pRT-TEVnIs-GUS-GFP, **(G)** pRT-VPgN-GUS-GFP, **(H)** pRT-VPg-GUS-GFP, **(I)** pROK2-AtFib2-mRFP, and **(J)** pROK2-AtU2B″-mRFP. pRT-GFP-NIa(E/H) with an amino acid substitution E189H in the internal cleavage site to prevent cleavage between the VPg and NIa-Pro domains was prepared by site-directed mutagenesis of pRT-GFP-NIa. NLS mutants (Figure 1) were prepared by site-directed mutagenesis of pRT-GFP-NIa and pRT-VPgN-GUS-GFP. The arrow represents the *Cauliflower mosaic virus* (CaMV) 35S promoter. Protein coding regions are marked by boxes.

addition to Lys-42 and Lys-44 and nuclear localization was not fully abolished by the aforementioned constructs, an additional construct was made to substitute all five Lys residues of the putative NLS region B with Ala. Whereas a substantial portion of the resultant protein VPgN(b)-GUS-GFP and GFP-NIa(b) remained in the cytoplasm, similar to the aforementioned B-site mutant proteins, a fraction of these proteins entered the nucleus (Figure 4I; see Supplemental Figure 1B online), indicating that another region at the N terminus of VPg contributed to nuclear localization.

We concluded that one of the additional putative NLS regions could be at the N terminus of VPg, which contains basic residues. The effect of the four N-terminal-most basic amino acid residues was studied, and the corresponding part of the N terminus was designated as region A (Figure 1). Substitution of the residues (Lys-4, Arg-5, Arg-7, and Lys-9) in this region with Ala significantly reduced, but did not abolish, nuclear localization of the resultant proteins VPgN(a)-GUS-GFP and GFP-NIa(a) (Figure 4H; see Supplemental Figure 1B online). When these substitutions in NLS region A were combined with the five substitutions made in the NLS region B, the resultant protein VPgN(ab)-GUS-GFP did not localize to the nucleus (Figure 4J). The two Lys residues (Lys-54 and Lys-55) in a region designated as C (Figure 1) were substituted with Ala [construct VPgN(bc)-GUS-GFP], which had no detectable effect on the already reduced nuclear localization of VPgN(b)-GUS-GFP (Figure 4K). As expected, no nuclear localization was observed for VPgN(abc)-GUS-GFP. These results indicated that the VPg domain of PVA NIa contains a bipartite NLS defined by region A (designated as NLS I) and region B (designated as NLS II).

NLS Regions in VPg Control Protein Targeting to the Nucleolus and CBs

Fluorescence from VPgN-GUS-GFP and GFP-NIa in the nucleus was concentrated in subnuclear bodies, presumably the nucleolus and CBs. The subnuclear bodies were identified using the fibrillarin 2 protein, which localizes to the nucleolus and CBs (Gall 2003), and the U2B″ protein, which localizes to CBs (Beven et al., 1995). The genes encoding these proteins were derived from *Arabidopsis thaliana*, and the subnuclear localization of the corresponding proteins in *N. benthamiana* has been reported (Kim et al., 2007b). The proteins were tagged with red fluorescent protein (AtFib2-mRFP and AtU2B″-mRFP) and coexpressed with VPgN-GUS-GFP, GFP-VPg, GFP-NIa, or GFP-NIa(E/H) in *N. benthamiana* leaves by agroinfiltration. The intensive green fluorescence from VPgN-GUS-GFP, GFP-VPg, GFP-NIa, and GFP-NIa(E/H) in a large nuclear body and smaller subnuclear bodies colocalized with the red fluorescence from AtFib2-mRFP (Figure 5A; see Supplemental Figure 3 online), indicating that the large body was the nucleolus and the smaller bodies were CBs. Red fluorescence from AtU2B″-mRFP colocalized with the smaller subnuclear bodies expressing GFP fluorescence from VPgN-GUS-GFP (Figure 5E), which confirmed that they were CBs.

VPgN(b)-GUS-GFP, in which the five Lys residues of NLS II (region B) were substituted with Ala, was not detected in the nucleolus (Figure 5B, Table 1). Substitution of two or three residues in NLS II (constructs b1N, b2N, b3N, and b4N; Figure 1) reduced but did not abolish nucleolar targeting. Among these mutants, the lowest rate of nucleolar localization was observed with Lys-42/Lys-44 substitutions (b1N and b3N), whereas mutants with a single Lys substitution (b2N and b4N) were not greatly affected (Table 1). Substitution of the four basic residues in NLS I (region A) with Ala abolished nucleolar targeting, as shown by expression and localization of VPgN(a)-GUS-GFP (Figure 5D). In accordance with these results, nucleolar localization of GFP-NIa(a) and GFP-NIa(b), containing substitutions at four and five residues of NLS I and NLS II, respectively, was reduced but to a lesser extent than with the corresponding fusion proteins containing the VPg N terminus only (see Supplemental Figure 3 online).

VPgN(b)-GUS-GFP still accumulated in CBs (Figures 5B and 5C), in contrast with VPgN(a)-GUS-GFP, which showed no signal in CBs (Figure 5D). These results were confirmed using AtU2B″-mRFP for colocalization (Figures 5F and 5G) and showed that NLS I directed protein localization to CBs.

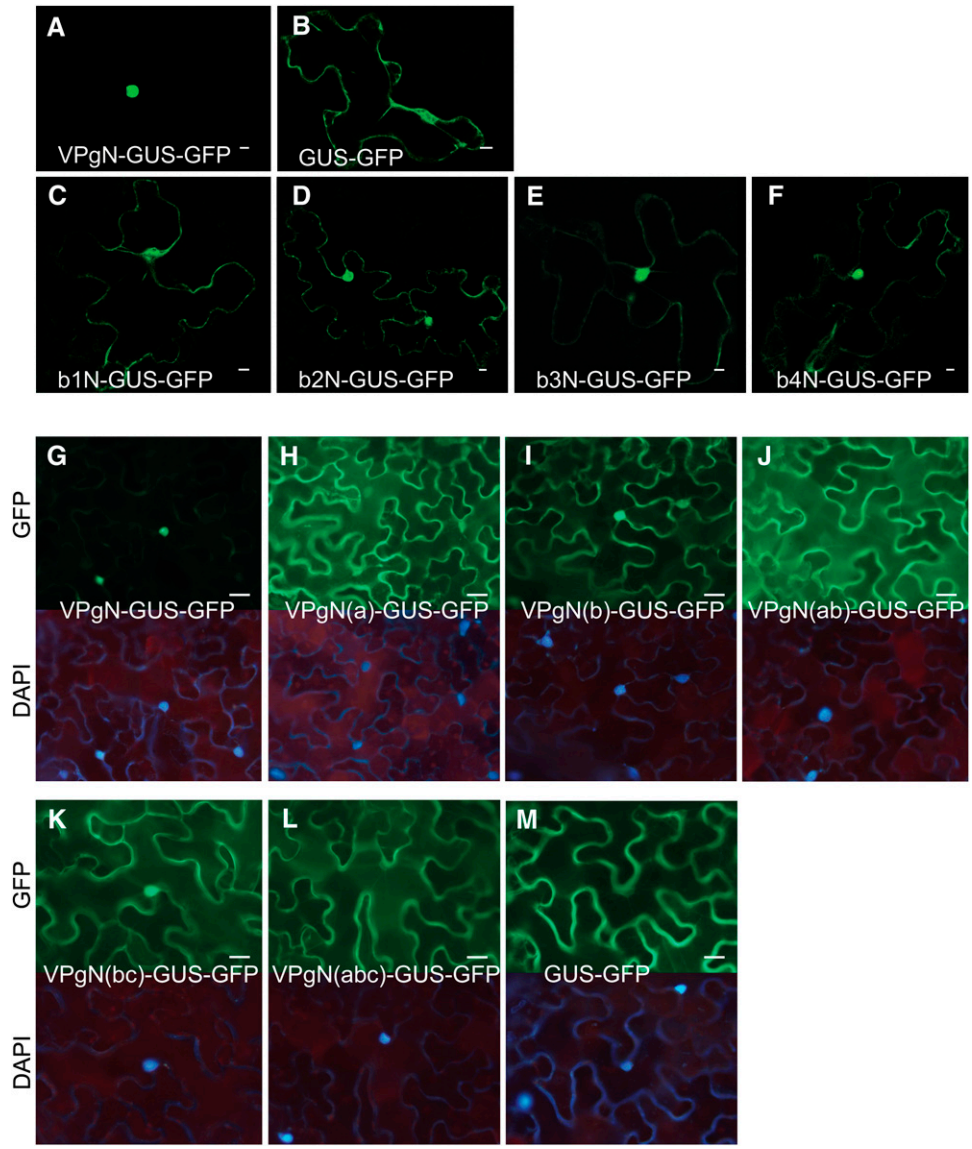

Figure 4. Subcellular Localization of GUS-GFP Fusion Proteins Carrying PVA VPg–Derived Sequences and the Effect of Mutations in NLS I and NLS II on Their Localization.

(A) to **(F)** Subcellular localization of GUS-GFP carrying N-proximal residues derived from PVA VPg as observed by confocal microscopy and shown as a single plane. Epidermal cells of *N. benthamiana* were bombarded for expression of VPgN(wt)-GUS-GFP (**[A]**; 55 N-proximal residues of VPg), GUS-GFP (**[B]**; no VPg-derived residues), or proteins in which two or three residues of the putative NLS region B of VPg (Figure 1A) were mutated: b1N-GUS-GFP **(C)**, b2N-GUS-GFP **(D)**, b3N-GUS-GFP **(E)**, or b4N-GUS-GFP **(F)**. These mutations reduced but did not abolish nuclear localization of the fusion protein. Bars = 10 μm.

(G) to **(M)** Effects of mutations in three putative NLS regions (A to C) of PVA VPg on nuclear localization of VPgN-GUS-GFP expressed in leaves of *N. benthamiana* by agroinfiltration and visualized by epifluorescence microscopy 3 DAIF. VPgN-GUS-GFP **(G)**, VPgN(a)-GUS-GFP **(H)**, VPgN(b)-GUS-GFP **(I)**, VPgN(ab)-GUS-GFP **(J)**, VPgN(bc)-GUS-GFP **(K)**, VPgN(abc)-GUS-GFP **(L)**, and GUS-GFP **(M)**. Specific mutations in regions A to and C are indicated in Figure 1A. DAPI staining was used to identify nuclei. Bars = 25 μm.

Interaction of PVA VPg with the Nucleolar Protein Fibrillarin

Fibrillarin is a major nucleolar protein also present in CBs (Gall, 2003). The ORF3 protein of GRV (Kim et al., 2007a) and some proteins of animal viruses interact with fibrillarin or certain other nucleolar proteins (reviewed in Hiscox, 2007), which prompted us to test whether PVA NIa could interact with fibrillarin. Two copies (Nb *Fib2a* and Nb *Fib2b*) of the fibrillarin gene were cloned from *N. benthamiana* and predicted to encode proteins of 314 residues differing at two positions (10 [S versus G, respectively] and 253 [M versus I, respectively]). The sequence of Nb *Fib2a*

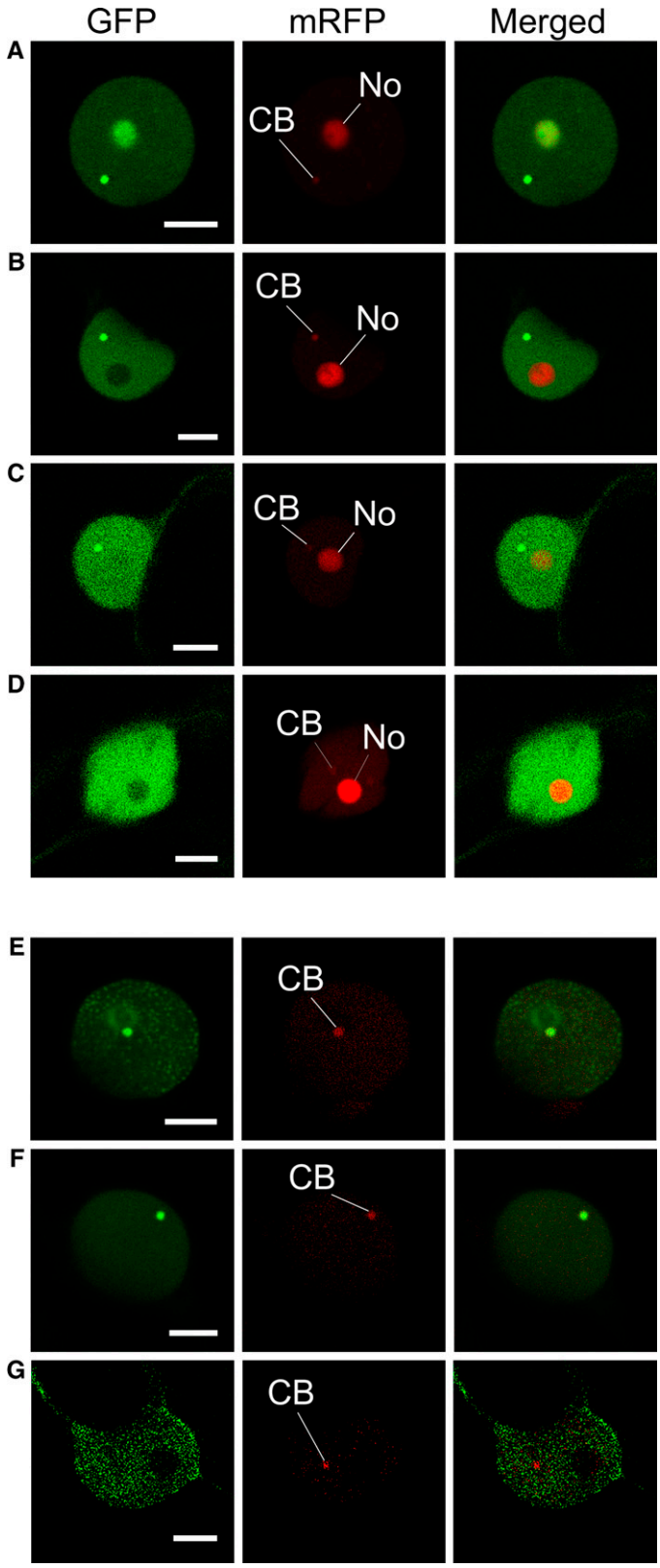

Figure 5. Subnuclear Localization of VPgN-GUS-GFP Fusion Protein Constructs Expressed in Leaves of *N. benthamiana* by Agroinfiltration and Detected by Confocal Microscopy 2 to 3 DAIF.

Table 1. Nucleolar Localization of VPgN-GUS-GFP Fusion Proteins

	Signals Detected in Nucleoli[b]		
Construct[a]	Strong	Detectable	Not Detected
VPgN	85%	14%	1%
VPgN(b)	0%	14%	86%
b1N	0%	48%	52%
b2N	5%	83%	12%
b3N	2%	45%	53%
b4N	3%	79%	18%

[a]In all constructs, the 55 N-proximal residues of PVA VPg were linked to the N terminus of the GUS-GFP marker protein fusion. VPgN indicates the wild-type VPg sequence. See Figure 1 for the identities of mutations introduced into the NLS region B of VPg in other constructs.

[b]A total of 136 to 225 epidermal cells of *N. benthamiana* in which GFP fluorescence was detected in the nucleoplasm were examined for fluorescence in the nucleolus by epifluorescence microscopy 2 to 3 DAIF.

was identical to the sequence available in the EMBL sequence database. Nb *Fib2a* and Nb *Fib2b* were inserted into yeast two-hybrid system (YTHS) vectors, and the respective proteins were found to interact with PVA VPg. Interaction was stronger with Nb Fib2b than Nb Fib2a (Figure 6). Mutations in NLS I (region A) or NLS II (region B) of VPg did not affect the interaction (Figure 6). Interactions were observed only when VPg was fused to the activation domain and Nb Fib2 to the binding domain of the YTHS vectors, which probably allowed normal folding of the proteins. All tested proteins were expressed at high levels in yeast (Figure 6C).

To study the interaction using an independent method, bimolecular fluorescence complementation (BiFC) was used. In BiFC, yellow fluorescent protein (YFP) is split into two nonfluorescent fragments, YN and YC. The possible interaction partners are fused with these fragments, which upon interaction of the two protein partners results in reconstruction of a fluorescent YFP (Zamyatnin et al., 2006). Nb Fib2 fused to YN and VPg fused to YC were transiently expressed in *N. benthamiana* leaves followed by observation of the leaves by epifluorescence microscopy 2 to 3 d after agroinfiltration (DAIF). The leaves infiltrated with YN-Nb Fib2 and VPg-YC showed strong fluorescence that was concentrated in small subnuclear bodies, identified as the nucleolus and CBs (see Supplemental Figure 4 online). Similar results were obtained when VPg and Nb Fib2 were fused to YN and YC, respectively. By contrast, only low-level fluorescence was observed when NLS I and NLS II mutants of VPg [VPg(a)-YC and VPg(b)-YC, respectively] were analyzed with YN-Nb Fib2 (see Supplemental Figure 4 online). This was not surprising as the NLS I and NLS II mutations dramatically reduced VPg accumulation in the nucleolus (Figure 5; see Supplemental Figure 3 online).

Mutations in the Two NLS Domains of VPg Reduce Virulence of PVA

The importance of NLS I and NLS II sequences in virulence of PVA was tested by introducing the aforementioned amino acid substitutions into the infectious cDNA of PVA and inoculating *N. benthamiana* and *N. tabacum* with the constructs by particle bombardment in up to four independent experiments. The mutant viruses PVA-a, PVA-b1, PVA-b2, PVA-b3, and PVA-b4 contained the mutations corresponding to VPgN(a), b1N, b2N, b3N, and b4N, respectively (Figure 1). The mutants PVA-b2 and PVA-b4, in which two residues (K42A and T45A, and K44A and T45A, respectively) were substituted in NLS II, infected the plants of *N. benthamiana* systemically at 8 d after inoculation (DAI), similar to the wild-type PVA (wtPVA) (Table 2). However, the concentration of the coat protein (CP) antigen with both mutants (229 to 290 $\pm$ 180 ng/g leaf tissue) was significantly lower than with wtPVA (701 $\pm$ 130 ng) (analysis of variance, $P = 0.001$), as determined by double antibody sandwich enzyme-linked immunosorbent assay (DAS-ELISA) using known amounts of purified PVA virions for comparison. Later, at 13 to 30 DAI, the CP concentrations of these mutants reached those of wtPVA in systemically infected leaves (Table 2). The symptoms caused by PVA-b2 and PVA-b4 were mild, and leaf malformation was not observed, whereas wtPVA caused severe leaf malformation and yellow chlorosis in systemically infected leaves. The mutated region was amplified from progeny viruses in systemically infected leaves by RT-PCR and sequenced, which revealed no reversion of mutated residues in PVA-b2 and PVA-b4.

When mutant PVA-a, containing four amino acid substitutions in NLS I, and mutant PVA-b1, containing two substitutions (K42A and K44A) in NLS II, were used to inoculate wild-type plants of *N. benthamiana*, no plant was systemically infected as tested by DAS-ELISA at 20 DAI (Table 2). Also, the inoculated leaves tested negative for virus. However, two wild-type plants were infected systemically with a third mutant, PVA-b3, in which three residues of NLS II were substituted (K42A, K44A, and T45A). Systemically infected leaves of the two plants contained low but readily detectable virus concentrations at 20 DAI (Table 2). Analysis of the mutated region from progeny viruses in systemically infected leaves by RT-PCR and direct sequencing revealed that PVA-b3 had retained the introduced mutations in one of

Figure 5. (continued).

Projections of two planes are shown. In **(A)** to **(D)**, fibrillarin (Fib2 of *Arabidopsis*) fused with red fluorescent protein (mRFP) was coexpressed with VPgN-GUS-GFP to visualize the nucleolus (No) and CBs.

(A) VPgN-GUS-GFP localizes to No and CBs.

(B) and **(C)** VPgN(b)-GUS-GFP with mutations in the NLS region B localizes to CBs but not to No.

(D) VPgN(a)-GUS-GFP with mutations in the NLS region A does not localize to No or CBs.

(E) to **(G)** The U2B″ protein of *Arabidopsis* fused with mRFP was coexpressed with VPgN-GUS-GFP to confirm the localization to CBs: VPgN-GUS-GFP **(E)**, VPgN(b)-GUS-GFP **(F)**, and VPgN(a)-GUS-GFP **(G)**. Bars = 5 μm.

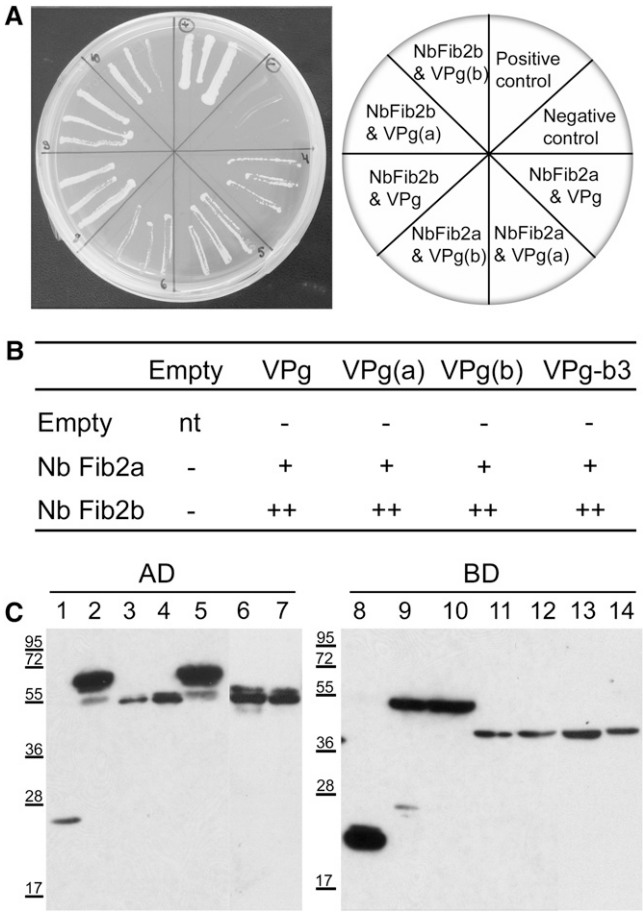

Figure 6. Interaction of PVA VPg with the Fibrillarin 2 Proteins Nb Fib2a and Nb Fib2b of *N. benthamiana* in YTHS.

Nb Fib2a and Nb Fib2b differ at two residues (10 [S versus G, respectively] and 253 [M versus I, respectively]).

(A) Differences in protein–protein interactions indicated by differences in the growth rate of yeast on the selection medium 8 d after plating.

(B) Relative differences in growth rate of yeast cotransformed for expression of different combinations of proteins: ++, growth in 2 to 4 d; +, growth in 5 to 8 d; –, no growth; nt, not tested.

(C) Immunodetection of the fusion proteins expressed in yeast by protein gel blotting using monoclonal antibodies to the GAL4 activation domain (AD) or DNA binding domain (DB). Lanes: 1, empty vector; 2, Nb Fib2a; 3, VPg; 4, VPg-b3; 5, Nb Fib2b; 6, VPg(a); 7, VPg(b); 8, empty vector; 9, Nb Fib2a; 10, Nb Fib2b; 11, VPg; 12, VPg-b3; 13, VPg(a); 14, VPg(b). The sizes of molecular mass markers (kD) are indicated to the left.

the two plants. In the other plant, VPg residue A45 had reverted back to Thr (wild type).

In *N. tabacum*, virulence of all mutant viruses tested was significantly compromised. Only one plant inoculated with PVA-b2 and three plants inoculated with PVA-b4 were systemically infected at 20 DAI, and virus concentrations were low (Table 2). The progeny viruses analyzed from the systemically infected leaves by RT-PCR and direct sequencing had retained the introduced mutations. No infection was detected with PVA-a, PVA-b1, and PVA-b3 (Table 2).

Expression of VPg Partially Complements an NLS Mutant of PVA in Transgenic Plants

Two transgenic lines of *N. benthamiana* (tt2 and tt7) expressing PVA VPg were inoculated with wtPVA and the mutants PVA-a, PVA-b1, PVA-b2, PVA-b3, and PVA-b4 to detect possible in trans complementation of the mutations. Little difference in systemic infection and virus accumulation was observed between wild-type, tt2, and tt7 plants following inoculation with wtPVA, PVA-b2, or PVA-b4, all of which showed high or relatively high levels of virulence (Table 2). Also, the low virulence of PVA-b3 and lack of detectable infectivity of PVA-a were not complemented in the transgenic lines compared with wild-type plants (Table 2). In two transgenic plants systemically infected with PVA-b3, the progeny viruses had retained the original mutations, but in two other plants, one of the three amino acid substitutions in VPg reverted to the wild type. The concentrations of wtPVA decreased from 13 to 20 DAI in the transgenic lines, probably because the initially high titers of PVA RNA and expression of the virus-homologous VPg transgene mRNA induced RNA silencing–based resistance to PVA, but no plant systemically infected with wtPVA or the aforementioned PVA mutants recovered from infection during the experiment until 28 DAI.

By contrast, infectivity of mutant PVA-b1 was noticeably improved in VPg-expressing transgenic plants. Although this mutant failed to infect any wild-type plant systemically, ~50% of the transgenic plants were systemically infected with virus titers no different from those of wtPVA at 20 DAI (Table 2). The progeny viruses were analyzed by RT-PCR and direct sequencing from systemically infected leaves, and in all cases PVA-b1 had retained the introduced mutations.

To exclude to some extent the possibility of mutations having occurred elsewhere in the viral genome, the NIb region was sequenced from viral progenies in 19 plants because NIa and NIb interact (Hong et al., 1995; Li et al., 1997; Guo et al., 2001). However, no mutations were found in NIb.

Mutations in the Two NLS Domains of VPg Reduce Multiplication of PVA in Protoplasts

The wtPVA, mutants PVA-b1, PVA-b2, PVA-b3, and PVA-b4, and an additional mutant, norPVA, with a frameshift in the open reading frame (to prevent any expression of CP from the PVA genome under the 35S promoter), were inoculated into protoplasts of *N. tabacum*. No PVA CP was detected in the protoplasts inoculated with PVA-b1, PVA-b3, or norPVA (Table 3). The mutants PVA-b2 and PVA-b4 multiplied to detectable levels, but the amounts of CP antigen were approximately fourfold and twofold lower than with wtPVA, respectively (Table 3).

Cosuppression of the *gfp* Gene in the Presence of VPg and NLS Mutants

Leaves of GFP transgenic *N. benthamiana* line 16c were coinfiltrated with *Agrobacterium tumefaciens* strains for expression of GFP and VPg, VPg(a) (K4A/R5A/R7A/K9A), VPg-b1 (K42A/K44A), VPg-b2 (K42A/T45A), VPg-b3 (K42A/K44A/T45A), VPg-b4 (K44A/T45A), or HC-Pro or GUS as controls. GFP

Table 2. Amounts of PVA CP Antigen in Systemically Infected Leaves of *N. benthamiana* and *N. tabacum* Inoculated with Wild-Type PVA and Mutants Containing Amino Acid Substitutions in Two NLSs Situated in the VPg Domain of NIa (NLS I and NLS II, Respectively, Separated by a Dash)

		wtPVA		PVA-b1		PVA-b2		PVA-b3		PVA-b4		PVA-a	
		KRQRQK - KKGKT		KRQRQK - K**A**G**A**T		KRQRQK - K**A**GK**A**		KRQRQK - K**A**G**AA**		KRQRQK - KKG**AA**		**AA**Q**A**Q**A** - KKGKT	
		n[a]	Amount (μg/g)[b]	*n*	Amount (μg/g)	*n*	Amount (μg/g)	*n*	Amount (μg/g)	*n*	Amount (μg/g)	*n*	Amount (μg/g)
N. benthamiana[c]													
8 DAI	wt	5/5	701 (±130)	0/5	–	4/5	229 (±180)	0/5	–	5/5	290 (±180)	0/19	–
	tt2	5/5	831 (±91)	0/5	–	5/5	181 (±150)	0/5	–	5/5	259 (±78)	0/10	–
	tt7	4/5	739 (±105)	0/5	–	2/5	271 (±257)	0/5	–	3/5	413 (±123)	0/10	–
13 DAI	wt	13/13	547 (±161)	0/13	–	12/13	375 (±173)	1/13	7.0	12/13	383 (±147)	0/19	–
	tt2	9/9	601 (±184)	6/11	127 (±202)	10/10	447 (±240)	0/11	–	10/10	388 (±108)	0/10	–
	tt7	9/10	621 (±235)	1/10	5.0	6/11	430 (±226)	2/10	556 (±181)	8/11	444 (±171)	0/10	–
20 DAI	wt	13/13	597 (±155)	0/13	–	11/13	490 (±123)	2/13	170 (±115)	13/13	462 (±105)	0/19	–
	tt2	9/9	272 (±165)	7/11	281 (±137)	10/10	418 (±108)	2/11	158 (±15)	10/10	327 (±91)	0/10	–
	tt7	9/10	240 (±179)	3/10	197 (±33)	7/11	370 (±118)	2/10	366 (±226)	7/11	299 (±94)	0/10	–
N. tabacum													
13 DAI	wt	13/13	9.4 (±4.4)	0/9	–	1/13	0.7	0/9	–	2/13	1.1 (±0.1)	0/5	–
20 DAI	wt	13/13	12.5 (±5.7)	0/9	–	1/13	6.9	0/9	–	3/13	2.6 (±1.6)	0/5	–

[a]The number of plants systemically infected as detected by DAS-ELISA among the total number of plants inoculated by particle bombardment in two experiments.

[b]Mean amounts of PVA CP antigen (μg/g leaf tissue) as determined by DAS-ELISA (SD in parentheses) using known amounts of purified PVA particles for comparison.

[c]Nontransgenic (wt) plants and plants of two VPg-transgenic lines (tt2 and tt7) of *N. benthamiana* expressing PVA VPg (Germundsson et al., 2007) were used.

fluorescence was readily visible in the leaf tissue coinfiltrated with GFP and VPg up to 4 d DAIF (Figure 7A) but faded thereafter. By contrast, GFP fluorescence was barely visible at any time in tissues infiltrated with GFP and VPg-a, VPg-b1, VPg-b2, VPg-b3, or VPg-b4, except for the fluorescence in veins due to the GFP expressed from the *gfp* transgene in the 16c line. Similarly, tissues coinfiltrated with GFP and GUS showed only temporal faint expression of GFP fluorescence, which started to decrease at 3 DAIF due to the expected activated *gfp* cosuppression. A bright red border eventually appeared around the infiltrated areas. Coinfiltration with GFP and HC-Pro resulted in strong and long-lasting GFP fluorescence (Figure 7A) that remained visible until the termination of the experiment (8 DAIF).

In the analyses done at 4 DAIF, the levels of GFP mRNA detected in tissues coinfiltrated with GFP and VPg or HC-Pro were higher than with GUS and GFP or GFP and VPg(a), VPg-b1, VPg-b3, VPg-b4 (Figure 7B), or VPg-b2. The *gfp*-specific small interfering RNAs (siRNAs) were detected in tissues infiltrated

Table 3. Infectivity of the PVA-nls Mutants in *N. tabacum* Protoplasts at 3 DAI

	Experiment 1		Experiment 2	
Virus[a]	Virus Amount (ng)[b]	Relative Amount	Virus Amount (ng)	Relative Amount
wtPVA	11.4 ± 0.9	100%	31.4 ± 3.6	100%
PVA-b1	0.0	0%	0.0	0%
PVA-b2	2.6 ± 1.6	23%	3.8 ± 0.5	12%
PVA-b3	0.0	0%	0.0	0%
PVA-b4	5.6 ± 0.6	49%	5.3 ± 0.3	17%
norPVA	0.0	0%	0.0	0%
Mock	0.0	0%	0.0	0%

[a]Recombinant PVA genomes used to inoculate protoplasts of *N. tabacum* by electroporation. The PVA mutants designated as b1 to b4 contain amino acid substitutions in the nuclear localization site B of the VPg domain of NIa. The amino acid substitutions are identical to those tested for their effect on nuclear and nucleolar localization of marker proteins (b1N to b4N) explained in Figure 1. wtPVA, wild-type PVA; PVAnor, a noninfectious PVA mutant obtained by introducing a frameshift mutation in the middle of the region encoding the first protein (P1) at the 5′-proximal part of the viral RNA; mock, protoplasts electroporated with buffer (no viral RNA).

[b]Mean amounts of PVA CP antigen (ng) per 10^6 inoculated protoplasts as determined by DAS-ELISA using known amounts of purified PVA particles for comparison. Relative amounts (%) were calculated by comparison with the amounts of wtPVA. Absorbance values (A_{405}) of norPVA and mock were 0.002 to 0.026.

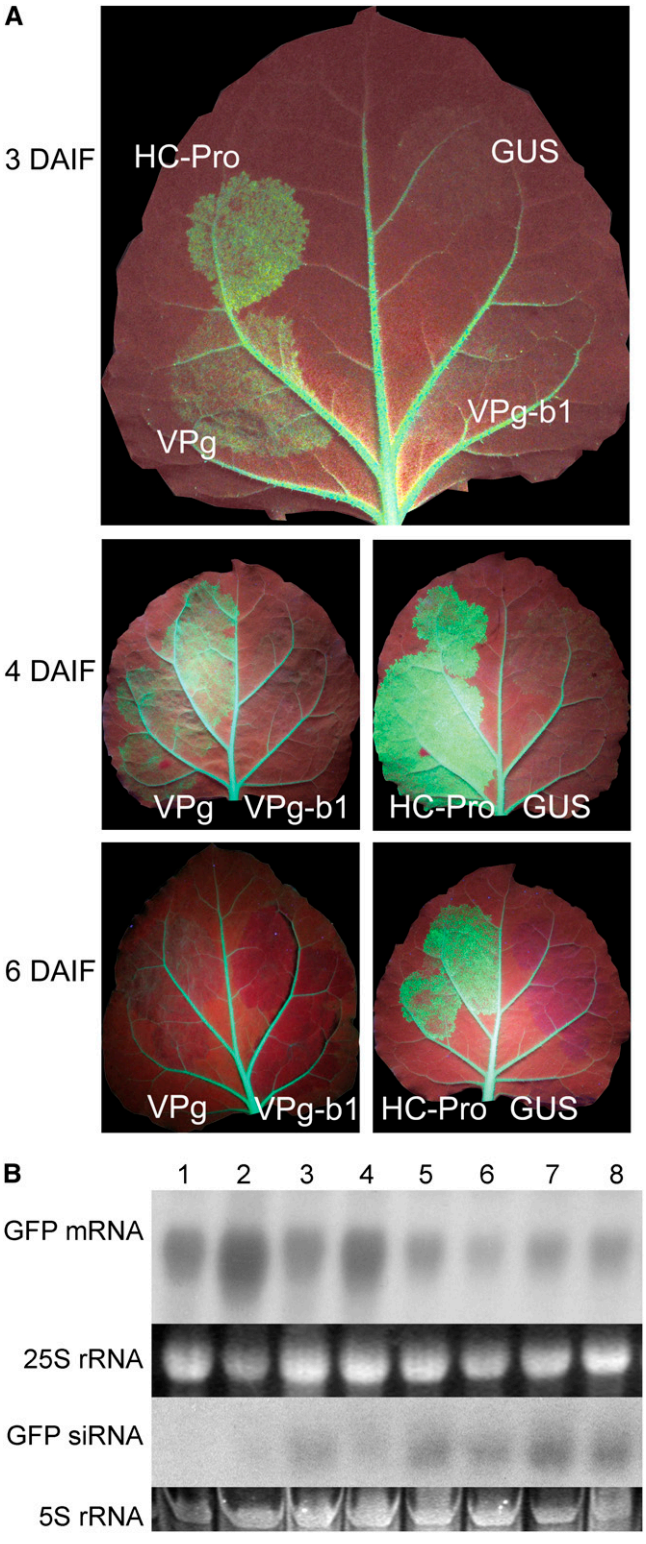

Figure 7. Interference with Cosuppression of the *gfp* Transgene by VPg and HC-Pro of PVA.

(A) Leaves of the *gfp*-transgenic *N. benthamiana* line c16 were coinfiltrated with *A. tumefaciens* strains expressing GFP and VPg or the mutated form of VPg-b1 (substitutions K42A and K44A) or GFP and HC-Pro or GUS. The undersides of the infiltrated leaves were photographed under UV light 3, 4, and 6 DAIF. Different leaves were photographed at 4 and 6 DAIF because leaves at 4 DAIF were used for RNA extraction.

(B) RNA gel blot analysis of *gfp* mRNA and *gfp*-specific siRNA from leaf tissues collected at 4 DAIF. Ethidium bromide staining of gels was used to control for equal loading. Lanes: 1, mock; 2, HC-Pro; 3, GUS; 4, VPg; 5, VPg(a); 6, VPg-b1; 7, VPg-b3; 8, VPg-b4.

with GFP and GUS, VPg(a), VPg-b1, VPg-b3, VPg-b4 (Figure 7B), or VPg-b2, but not in tissues infiltrated with GFP and VPg or HC-Pro (Figure 7B). Only low levels of *gfp*-specific siRNA were detected in tissues coinfiltrated with GUS and GFP at 4 DAIF, which was probably because cosuppression had only recently initiated and GFP expression levels were low. The experiment was performed two to five times with wild-type VPg and different VPg mutants, and results were similar each time.

Fibrillarin Silencing Reduces PVA Accumulation

To examine whether fibrillarin plays a role in PVA infection, as it does in infection of GRV (Kim et al., 2007a), fibrillarin expression was suppressed in *N. benthamiana* plants using a *Tobacco rattle virus* (TRV)-based vector carrying a fragment of the Nb *Fib2a* gene of *N. benthamiana* (TRV-Fib2). *N. benthamiana* plants were also inoculated with an empty TRV vector as a control. To monitor initiation of silencing, a few plants were inoculated with the TRV vector carrying a fragment of the phytoene desaturase gene (TRV-PDS), which provides a silencing phenotype characterized by loss of chlorophyll (Ratcliff et al., 2001). At the time point when PDS silencing was manifested in plants inoculated with TRV-PDS (see Supplemental Figure 5 online), the mean expression level of fibrillarin mRNA in the leaves of TRV-Fib2–infected plants was ~25 to 86% (n = 6) that of the leaves in the corresponding position of TRV-infected plants, as determined by real-time RT-PCR (see Supplemental Figure 6 online). The top leaves of plants systemically infected with TRV-Fib2 exhibited severe curling and malformation, which resulted in severe stunting of the plants (see Supplemental Figure 5 online). Therefore, the lower, nearly fully expanded upper leaves exhibiting the aforementioned depletion of Nb *Fib2* expression were mechanically inoculated with PVA, and leaves at the corresponding position in TRV-infected control plants were inoculated as controls. PVA accumulation was 52 to 66% in the inoculated leaves of fibrillarin-silenced plants compared with nonsilenced TRV-infected control plants as tested 6 DAI in three experiments (Table 4). PVA was also detected in the upper noninoculated leaves in both types of plants, and differences in virus concentration between fibrillarin-silenced and nonsilenced upper leaves were similar to those observed in inoculated leaves (Table 4).

DISCUSSION

Our data show that nuclear localization of NIa is controlled by residues 4 to 9 (NLS I) and 41 to 50 (NLS II) of the VPg domain in PVA. Both regions were needed for efficient nuclear localization,

Table 4. Amounts of PVA CP Antigen in the Inoculated and Upper Noninoculated Leaves of Fibrillarin-Silenced and Nonsilenced *N. benthamiana* Plants at 6 DAI

	Inoculated Leaves			Upper Noninoculated Leaves		
	n[a]	Amount (μg/g)[b]	Relative Amount[c]	*n*	Amount (μg/g)	Relative Amount
Experiment 1						
Nonsilenced[d]	4/4	95.3 (±33.5)	100%	4/4	222.0 (±23.4)	100%
Fib-silenced[e]	4/4	62.9 (±46.4)	66%	2/4	62.7 (±4.8)	28%
Experiment 2						
Nonsilenced	12/12	264.1 (±49.8)	100%	12/12	280.1 (±63.1)	100%
Fib-silenced	12/12	136.1 (±54.1)	52%	10/12	183.9 (±91.5)	66%
Experiment 3						
Nonsilenced	4/4	95.2 (±65.9)	100%	4/4	186.3 (±18.3)	100%
Fib-silenced	5/5	55.1 (±34.5)	58%	4/5	87.3 (±89.2)	47%

[a]The number of PVA-infected leaves among the total number of leaves sap-inoculated with PVA. Viral CP antigen was detected by DAS-ELISA.
[b]Mean amounts of PVA coat protein antigen (μg/g leaf tissue) as determined by DAS-ELISA (SD in parentheses) using known amounts of purified PVA particles for comparison. Amounts of PVA were significantly lower in the inoculated and upper noninoculated leaves of Fib-silenced plants than in the corresponding nonsilenced leaves in the three experiments (experiments 1 to 3; *t* test, P = 0.001).
[c]Relative amounts of PVA CP antigen between nonfibrillarin-silenced and silenced tissues.
[d]Plants infected with TRV vector carrying no heterologous insert.
[e]Plants infected with a TRV vector containing a fragment of the Nb *Fib2a* gene. Silencing was likely to affect both Nb *Fib2a* and Nb *Fib2b* expression because the gene fragment used for silencing derived from Nb *Fib2a* was 97.3% identical to that derived from Nb *Fib2b*.

and NLS I seemed particularly important (Figure 4; see Supplemental Figure 1B online). These results provide further evidence for a bipartite NLS in potyviral NIa. In a previous study, the NIa of TEV was expressed in transgenic *N. tabacum* plants, and as with PVA in our study, the region corresponding to NLS II was found to control nuclear localization (Carrington et al., 1991; Schaad et al., 1996). In addition, data suggested that the N-terminal residues of NIa contributed to optimal nuclear localization of TEV NIa (Carrington et al., 1991). Hence, results for these two potyviruses are consistent with regard to the existence of NLS I and NLS II in the VPg domain. Moreover, both NLS regions are highly conserved in genus *Potyvirus* (see Supplemental Figure 7 online).

Our results also show that NLS I and NLS II control nucleolar localization of PVA NIa. Mutation of one of the two NLS regions was sufficient to abolish nucleolar targeting, unlike the situation for nuclear localization. Secondly, nucleolar targeting was reduced and eventually abolished by an increasing number of basic residue substitutions (Lys residues replaced by Ala) in NLS II, whereas nuclear localization was similarly reduced but not abolished by these mutations (Table 1, Figures 4 and 5; see Supplemental Figures 1B and 3 online). Hence, nucleolar and nuclear localization were controlled independently by the same NLS regions. Although TEV NIa has been observed in the nucleolus (Schaad et al., 1996), detailed studies on nucleolar targeting of NIa have not been reported. Thus, our current findings on nucleolar and nuclear localization of a potyviral protein were made in a study area that has generally gained little attention in plant virology (Kim et al., 2007a, 2007b).

PVA NIa was found to accumulate in CBs, which are highly dynamic structures originally described as nucleolar accessory bodies (reviewed in Pontes and Pikaard, 2008). Localization to CBs was controlled by NLS I, whereas mutations in NLS II had little effect. Hence, mutations in NLS II prevented nucleolar localization but allowed high levels of accumulation in CBs. This was particularly pronounced in experiments involving only the N-proximal part of VPg fused to marker proteins. Similar results were obtained using NIa, but the lower intensity of signals in CBs using these constructs made comparison of differences more difficult.

There is only a single precedent of a plant virus protein localized in CBs. The ORF3 protein of GRV (unrelated to potyviruses) accumulates in nucleoli and CBs where it interacts with fibrillarin (Kim et al., 2007a, 2007b), a major nucleolar protein also present in CBs (Gall, 2003). It was therefore relevant to test for possible interactions between NIa and fibrillarin. Data showed that the VPg domain of PVA NIa interacted with fibrillarin in vivo. This interaction was detected initially by YTHS and subsequently studied in plant cells by BiFC. In GRV, interaction between the ORF3 protein and fibrillarin recruits some fibrillarin to the cytoplasm for assembly of virus-like particles that are competent for long-distance movement (Kim et al., 2007a, 2007b; Canetta et al., 2008). However, it seems unlikely that the interaction between VPg and fibrillarin would recruit fibrillarin to the cytoplasm because the interaction between VPg and fibrillarin was observed only in nucleoli and CBs but not in the cytoplasm. Another difference was observed in nucleolar trafficking of PVA NIa and GRV ORF3. Whereas ORF3 uses a mechanism that involves the appearance of multiple CB-like structures followed by fusion of these structures with nucleoli (Kim et al., 2007a, 2007b), no multiple CB-like structures were observed with NIa or mutated NIa proteins. Despite these differences, results with PVA NIa and GRV ORF3 both indicate that interactions of these viral proteins with fibrillarin are important for virus infection; the underlying mechanism, however, may differ. Reduction of fibrillarin expression by ~30 to 80% in leaves by means of virus-induced gene silencing (VIGS) reduced PVA accumulation by

~50% but did not prevent systemic spread of the virus. In similar experiments with GRV, fibrillarin depletion was manifested as inhibition of systemic spread of the virus (Kim et al., 2007a, 2007b).

Substitution of the basic amino acids Lys-42 and Lys-44 with Ala in NLS II caused the greatest reduction of nucleolar localization and the greatest loss of virulence in PVA in *Nicotiana* plants (Tables 1 to 3). For example, the mutant viruses PVA-b1 and PVA-b3 failed to multiply in *N. tabacum* protoplasts. These negative effects on virulence may have been caused by the lack of nucleolar localization; still, residues in the NLS II region defined in this study have also been implicated in NTP binding and uridylylation of PVA VPg (Puustinen and Mäkinen, 2004). However, the region of VPg defined as NLS I in this study has not been implicated in any other potyviral functions. Mutations in NLS I inhibited nucleolar and CB localization of NIa and infection of *N. tabacum* and *N. benthamiana* plants. A larger part of the N terminus of VPg (16 residues) has been implicated in interactions with a plant protein, PVIP, that contains a motif common to proteins involved in transcriptional regulation via chromosome remodeling (Dunoyer et al., 2004). These findings from independent experiments link nucleolar localization of NIa and the corresponding regions of the VPg domain with important viral functions.

The severely debilitated functions of PVA-b1 (Lys-42 and Lys-44 mutated to Ala in NLS II) were complemented by the wild-type VPg expressed in transgenic lines of *N. benthamiana*, which was not observed with PVA-b3 that carried a third mutation (T45A). These findings are essentially novel because functional defects due to mutations in VPg are usually not complemented in trans (Schaad et al., 1996, 1997; Nicolas et al., 1997; Keller et al., 1998; Rajamäki and Valkonen, 1999). Only in one study was multiplication of a TEV mutant containing the amino acid substitutions analogous to PVA-b1 stimulated in protoplasts of a transgenic *N. tabacum* line expressing the wild-type 6K2/NIa polyprotein of TEV (Schaad et al., 1996). It seems that Lys-42 and Lys-44 in the PVA NIa control a specific function that is distinct from other functions by complementation in trans. We hypothesized that the function could be related to circumvention or suppression of host defense because the PVA-b2 and PVA-b4 mutants substituted only for one of the two residues (Lys-42 or Lys-44) showed reduced amplification but were able to mediate systemic infection in a large proportion of inoculated plants. The virulence of these mutants was also more severely reduced in *N. tabacum* than *N. benthamiana*, consistent with studies showing that *N. tabacum* is more resistant to viruses than *N. benthamiana* (Yang et al., 2004; Rajamäki et al., 2005). Alternatively, an interaction with host factors controlled by Lys-42 and Lys-44 of NIa may stimulate host functions necessary for viral infection. Interaction of NIa with eIF(iso)4E has been observed in the nucleus (Beauchemin et al., 2007); however, we did not consider this relevant because to our knowledge, the interaction between PVA NIa with eIF(iso)4E is not affected by the aforementioned substitutions in NIa.

The hypothesis that nuclear localization of VPg/NIa might play a role in interference with host antiviral defense was supported by the finding that VPg interfered with *gfp* cosuppression and was hence able to control gene silencing, a mechanism involved in regulation of cellular gene expression and antiviral defense (Pontes and Pikaard, 2008; Ruiz-Ferrer and Voinnet, 2009). While the ability of VPg to suppress gene silencing was temporal and weaker than that of HC-Pro, the well-known gene silencing suppressor of potyviruses (Brigneti et al., 1998; Johansen and Carrington, 2001), it was consistently observed in five independent experiments. It therefore seems that VPg is an auxiliary factor involved in interference of RNA silencing by potyviruses. This effect of VPg was absent in similar experiments performed in a previous study probably because the mRNAs for GFP and VPg expression both included the PVA 5′-untranslated region and the homologous sequences added to the silencing pressure (Germundsson et al., 2007). Previous studies have implied that the P1 protein of potyviruses also acts as an auxiliary factor for suppression of RNA silencing (Rajamäki et al., 2005).

RNA silencing is an inducible antiviral defense mechanism of particular importance in plants; therefore, impaired PVA infectivity following mutations that abolish any detectable effects of VPg on gene cosuppression is consistent with involvement of VPg in suppression of RNA silencing during virus infection. The infectivity of PVA carrying some of these mutations in VPg was complemented in trans in transgenic plants expressing wild-type VPg, which was to be expected if the mutations compromised suppression of RNA silencing; the viral proteins capable of suppressing RNA silencing have so far been identified mainly by assays where they are expressed in trans outside the infection context (Díaz-Pendón and Shou-Wei, 2008). Previous studies show that VPg is transported from lower infected leaves and accumulates in the companion cells in sink leaves prior to systemic infection, which was hypothesized to be needed for suppression of host defense and initiation of infection (Rajamäki and Valkonen, 2003). Results of this study are consistent with this hypothesis and suggested that the mutations, and hence VPg/NIa, played a major role at an early phase of infection because mutations severely compromised infectivity. However, once infection was established in inoculated leaves, the mutants were able to infect the plants systemically, which suggests that the proposed auxiliary functions of VPg in silencing suppression are not an absolute requirement for infection in *N. benthamiana.*

Studies on mutated forms of VPg showed that suppression of silencing was linked to localization to the nucleus, nucleoli, and CBs. These findings on the linkage between VPg nuclear localization and its silencing suppression function also seem conceivable based on the pivotal roles of nucleoli and CBs as processing centers for small RNAs, including siRNAs and microRNAs that regulate gene expression posttranscriptionally (Pontes et al., 2006; Brosnan et al., 2007; Pontes and Pikaard, 2008). siRNA and CBs are also involved in transcriptional gene silencing by methylation (Pontes and Pikaard, 2008). There are a few previous examples of viral proteins whose activity in suppression of RNA silencing depends on nuclear localization. The 2b protein of *Cucumber mosaic virus* (Bromoviridae) and P0 protein of *Beet western yellows virus* (Luteoviridae) interact with Argonaute1, the core component of the RNA-induced silencing complex, in the nucleus and inhibit its activity or target it for degradation, respectively (Zhang et al., 2006; Bortolamiol et al., 2007). The P6 protein of CaMV (Caulimoviridae) inhibits the nuclear protein DRB4,

which is required for siRNA synthesis by Dicer-like protein 4 (Haas et al., 2008). The large number of host proteins known to be involved in regulation of RNA silencing in the nuclear environment (e.g., siRNA and microRNA processing in nucleoli and CBs; Pontes and Pikaard, 2008) makes it challenging to identify the host factors targeted by VPg for interference with silencing. Fibrillarin is included in small nuclear and nucleolar ribonucleoproteins that accumulate in CBs en route to spliceosomes and nucleoli, respectively (Pontes and Pikaard, 2008), also suggesting a role for the fibrillarin–VPg interaction in silencing suppression. Alternatively, the fibrillarin–VPg interaction may disrupt certain nucleolar functions (e.g., host transcription or pre-mRNA processing), which might explain the observed shutdown of host gene expression during potyvirus infection (Wang and Maule, 1995). Because VPg seems to suppress silencing in the nuclear environment, we hypothesize that its main target is a host gene. By contrast, many previously described viral silencing suppressors function in the cytoplasmic environment to sequester virus-derived siRNA (Díaz-Pendón and Shou-Wei, 2008; Ruiz-Ferrer and Voinnet, 2009).

Our study provides evidence that the successful infection cycle of the picorna-like potyvirus PVA requires localization of viral VPg/NIa to the nucleus, nucleoli, and CBs, which may be a consequence of the need to interfere with host defenses and hence facilitate initiation of infection. These findings are supported by studies indicating that nuclear localization of NIa is needed for successful infection by TEV (Schaad et al., 1996) and that poliovirus (family Picornaviridae) regulates nuclear and nucleolar functions in host cells (Waggoner and Sarnow, 1998; Izumi et al., 2001; Hiscox, 2003; Banerjee et al., 2005). Hence, the results reported here may be generally applicable to a large number of picorna-like plant and animal viruses.

METHODS

Plant Material

Plants of tobacco (*Nicotiana tabacum* cv Samsun nn), *Nicotiana benthamiana*, and transgenic *N. benthamiana* lines tt2 and tt7 expressing the VPg of PVA (Germundsson and Valkonen, 2006) were grown from seeds of our own stock. Seeds of the transgenic line 16c of *N. benthamiana* showing strong constitutive expression of GFP (Brigneti et al., 1998) were kindly provided by David Baulcombe. Plants were grown in a growth chamber (Weiss Umweltstechnik) under constant conditions (photoperiod 16 h; light intensity 250 μE s^{-1} m^{-2}; temperature 22/18°C day/night; relative humidity 75%) and watered daily as needed and fertilized weekly with 1% fertilizer (N:P:K = 16:9:22; Puutarhan täyslannos, Kemira GrowHow).

Construction of Mutant PVA cDNAs

Recombinant PVA cDNA clones were constructed based on a vector containing the full-length infectious cDNA clone of PVA-B11 placed under the control of the *Cauliflower mosaic virus* (CaMV) 35S promoter (Puurand et al., 1996). Mutations were introduced into the VPg coding sequence to substitute basic residues or a Thr residue in the putative NLS regions with Ala. Site-directed mutagenesis of the VPg coding sequence was performed on a plasmid containing a 1898-nucleotide-long *Hin*dIII-*Apa*I fragment of the PVA cDNA (Figure 1) as described (Rajamäki and Valkonen, 1999) using the QuickChange site-directed mutagenesis system (Stratagene) and appropriate nucleotide primers (see Supplemental Table 1 online). Mutations were verified by sequencing. Subsequently, a 1208-nucleotide-long fragment of the mutated sequence was released by digestion with *Swa*I and *Apa*I and transferred to the unique *Swa*I and *Apa*I sites in the full-length PVA cDNA (Figure 1) as described (Rajamäki and Valkonen, 1999). PVA mutant PVA-a contained four amino acid substitutions (K4A, R5A, R7A, and K9A) in NLS I in VPg. PVA-mutants PVA-b1 (K42A and K44A), PVA-b2 (K42A and T45A), PVA-b3 (K42A, K44A, and T45A), and PVA-b4 (K44A and T45A) have two to three amino acid substitutions in NLS II in VPg (Figure 1). PVAnor contains the *GFPuv* sequence in a reverse orientation inside the P1 gene and was constructed as described (Rajamäki et al., 2005).

Transient Protein Expression in Leaf Cells from Vectors Introduced by Particle Bombardment

The recombinant clones to be introduced into plant cells for transient expression by particle bombardment were constructed in the pRT-GFP plasmid (Solovyev et al., 2000) kindly provided by Andrey Zamyatnin (Swedish University of Agricultural Sciences, Uppsala, Sweden), except the constructs for expression of GFP-VPg and GFP-NIa, which were based on the plasmid pRT-GFP/TGBp1 (Zamyatnin et al., 2004). All plasmid transcriptions were under the control of the CaMV 35S promoter and terminated by the polyadenylation signal. Standard cloning procedures were used (Sambrook and Russell, 2001). The resulting clones were verified by restriction enzyme digestion and sequencing. Plasmids were cloned in *Escherichia coli* DH5α.

To construct pRT-GFP-NIa, pRT-GFP-NIa(a), pRT-GFP-NIa(b1), pRT-GFP-NIa(b2), pRT-GFP-NIa(b3), and pRT-GFP-NIa(b4), the NIa coding region was amplified from the corresponding infectious PVA cDNA by PCR with primers specific for the 5′-end and 3′-end of the NIa coding sequence and which contained a *Bam*HI site and a *Xba*I site, respectively (see Supplemental Table 1 online). The 3′-end primer also included a TAA translation stop codon at the end. The PCR products were digested with *Bam*HI and *Xba*I and cloned in the pRT-GFP/TGBp1 vector digested with the same enzymes, which yielded plasmids with the NIa fused to the C terminus of GFP. pRT-GFP-VPg was produced as above but using a reverse primer specific to the 3′-end of the VPg coding sequence. The internal proteolytic processing site of NIa was mutated in pRT-GFP-NIa by replacing the Glu residue in the internal cleavage site by His (E189H) using appropriate primers. The resulting construct was named pRT-GFP-NIa(E/H).

To prepare pRT-GUS-GFP, a DNA fragment containing the full-length GUS gene sequence was PCR amplified from pA-GUS (Savenkov and Valkonen, 2001) using primers specific to the 5′-end and 3′-end of the GUS sequence (see Supplemental Table 1 online). The 5′-end primer included an AUG translation initiation codon and a unique *Kpn*I restriction site, whereas the 3′-end primer included a unique *Nco*I restriction site but lacked the GUS stop codon. The PCR fragment was digested with *Kpn*I and *Nco*I and cloned into a similarly digested pRT-GFP vector to yield plasmid pRT-GUS-GFP, in which the N terminus of GFP was fused to GUS.

pRT-PVAnls-GUS-GFP and pRT-TEVnls-GUS-GFP (Figure 3) were constructed as above but using a forward primer containing a *Kpn*I restriction site and initiation codon (AUG) followed by the nucleotide sequence for 10 amino acids of the putative PVA VPg NLS II (residues 41 to 50 of PVA VPg; region B in Figure 1) or the TEV VPg NLS (residues 40 to 49 of TEV VPg; Figure 1B) (Schaad et al., 1996), respectively, and the GUS 5′-end sequence.

To make pRT-VPg-GUS-GFP, the full-length VPg sequence was amplified by PCR with primers that contained an *Xho*I or a *Kpn*I site and were specific to the 5′-end and 3′-end of the VPg coding sequence, respectively. The 5′-end primer also included an AUG translation initiation codon before the VPg sequence. The PCR product was digested with *Xho*I and

*Kpn*I and cloned into a similarly digested pRT-GUS-GFP vector, yielding a plasmid with the VPg fused to the N terminus of GUS-GFP. pRT-VPgN-GUS-GFP was constructed essentially as pRT-VPg-GUS-GFP but using a 3′-end primer that annealed to a sequence at nucleotides 146 to 165 downstream from the NLS II region in VPg. When expressed this construct produced the first 55 residues of VPg fused to the N terminus of GUS-GFP.

To express fusion proteins in which residues in the NLS I and NLS II regions in VPg were substituted with Ala, the sequence encoding the N-proximal region of VPg (residues 1 to 55) was amplified from the mutated PVA cDNAs (PVA-a, PVA-b1, PVA-b2, PVA-b3, and PVA-b4) and inserted into pRT-GUS-GFP. The resultant plasmids were designated as pRT-VPgN(a)-GUS-GFP, pRT-b1N-GUS-GFP, pRT-b2N-GUS-GFP, pRT-b3N-GUS-GFP, and pRT-b4N-GUS-GFP, respectively (Figures 1 and 3).

Constructs pRT-VPgN(b)-GUS-GFP and pRT-GFP-NIa(b), in which all basic residues of NLS II were substituted with Ala, were made by site-directed mutagenesis of the VPg coding sequence in the plasmid pRT-b1N-GUS-GFP and pRT-GFP-NIa(b1), respectively, using appropriate primers as described above. The VPg sequence in pRT-VPgN(b)-GUS-GFP was subjected to further site-directed mutagenesis to obtain the constructs pRT-VPgN(ab)-GUS-GFP, pRT-VPgN(bc)-GUS-GFP, and pRT-VPgN(abc)-GUS-GFP, which contained additional amino acid substitutions in two or three putative NLS regions (A, B, and C; Figure 1).

Plasmid DNA was precipitated on tungsten particles (Bio-Rad) by first adding 18 μL of tungsten particles (60 mg/mL) to plasmid DNA (5 to 10 μg) under continuous mixing in a total volume of 40 μL and then adding one-tenth volume of 3 M sodium acetate and 3 volumes of absolute ethanol. After incubation at –20°C for 1 h, the samples were centrifuged at 2000*g* for 30 s and washed carefully three times with absolute ethanol. Full-grown leaves were detached from 6- to 8-week-old *N. benthamiana* plants, placed on moist Whatman paper in a Petri dish, and inoculated by particle bombardment using the PDS-100 system (Bio-Rad) as described (Morozov et al., 1997).

Protein Expression in Leaves Using Agroinfiltration

For transient protein expression in leaves by agroinfiltration, binary vectors were prepared by transferring the aforementioned expression cassettes from the pRT vectors to the binary vector pKOH200 (Savenkov and Valkonen, 2001). The pRT vectors were digested with *Hin*dIII, which releases the expression cassette including the 35S promoter from the pRT vector backbone. The cassette was subsequently ligated to pKOH200 linearized with *Hin*dIII.

Binary vectors were electroporated into *Agrobacterium tumefaciens* strain C58C1 (Ti plasmid pGV2260) using a Bio-Rad Gene Pulser. For transient expression of the constructs, the underside of a leaf of *N. benthamiana* was infiltrated essentially as described by Llave et al. (2000). Briefly, the *Agrobacterium* cultures were grown in Luria broth with appropriate antibiotic selection at 28°C for 16 h. The cells were collected by centrifugation and resuspended in infiltration medium (10 mM $MgCl_2$ and 20 μM acetosyringone) to an OD_{600} 0.4 to 0.6 and incubated at room temperature for 3 h before injection into leaves. For colocalization of two proteins, the cultures of the corresponding two *A. tumefaciens* strains were combined in a 1:1 ratio (v/v) for infiltration.

Fluorescence Microscopy

Epifluorescence microscopy was done with a Leitz Laborlux 12D microscope with an epifluorescence extension (Leitz Ploemopak) and the appropriate filters (Leica Nilomark Oy) on samples stained with DAPI, expressing GFP fusion proteins or expressing YFP fluorescence resulting from BiFC. Confocal microscopy was used to study subcellular localization of the GFP- and mRFP-tagged proteins and detect protein–protein interactions by BiFC. The microscopy was performed with a Leica TCS SP2 AOBS device using ×20 and ×63 water immersion objectives at the Institute of Biotechnology, University of Helsinki.

VIGS

To suppress expression of fibrillarin in *N. benthamiana* by VIGS, a *Tobacco rattle virus*–based vector was used (kindly provided by David Baulcombe). A 441-bp fragment from the 5′-end of Nb *Fib2a* was PCR amplified from pGAD-Fib2a using appropriate primers and cloned into the *Sma*I site of TRV RNA2 vector pTV00 (Ratcliff et al., 2001). The vector named pTV-Fib2 was transformed into *A. tumefaciens* GV3101 containing pSa-rep. To induce VIGS, *A. tumefaciens* strains carrying TRV RNA1 (pBINTRA6) and RNA2 (pTV00, pTV-Fib2, or pTV-PDS) were combined in a ratio of 1:1 (v/v) and agroinfiltration was performed as above.

Virus Inoculation and Detection in Plants

Plants of *N. benthamiana* and *N. tabacum* were inoculated with PVA cDNA clones using the Helios Gene Gun System (Bio-Rad). Plasmid DNA was linearized by *Age*I digestion. Cartridges were prepared and used for bombardment of leaves as described (Hämäläinen et al., 2000). The first full-grown leaves were inoculated when plants were 5 to 6 weeks old. The upper leaves of *N. benthamiana* plants used for VIGS assays were Carborundum dusted and mechanically inoculated with sap extracted from PVA-infected plants.

PVA was detected in the inoculated and upper noninoculated leaves by DAS-ELISA using a monoclonal antibody (MAb 58/0; Adgen) and an alkaline phosphatase–conjugated MAb 58/0 to PVA CP as described (Rajamäki et al., 1998). Samples were weighed and ground in ELISA sample buffer at 1 g per 10 mL. Leaf samples from *N. benthamiana* were further diluted 100-fold. Two 100-μL aliquots from each sample were transferred to an ELISA microtiter plate (Greiner Laborteknik) coated with MAb 58/0. Known amounts of purified PVA particles (0.32 to 200 ng) were included in all ELISA plates as a standard to estimate PVA concentrations in leaves.

For sequencing the mutated genomic regions in virus progeny, PVA virions were immunocaptured from leaf sap prepared as described for DAS-ELISA. A microcentrifuge tube was coated with the PVA MAb 58/0, and 100 μL of sap was added followed by incubation at 4°C overnight. cDNA synthesis on viral RNA was performed using *Moloney murine leukemia virus* reverse transcriptase (Promega) and random hexamers [$(dN)_6$] according to the manufacturer's instructions. Viral sequences were amplified by PCR using primers targeted to the 3′-ends of the cylindrical inclusion protein (CI) and VPg encoding regions or of the 5′- and 3′-ends of the NIb region, followed by direct sequencing of the PCR products.

Preparation and Inoculation of Protoplasts

Protoplasts were prepared from mature leaves of *N. tabacum*. PVA cDNA (7 μg) was introduced into batches of 10^6 protoplasts by electroporation with a Bio-Rad Genepulser II as described (Denecke and Vitale, 1995) except that the electroporation buffer of Salmenkallio-Marttila et al. (1995) was used. Electroporated protoplasts were incubated at room temperature under dim light for 2 to 3 days, after which they were harvested by low-speed centrifugation (2000*g* for 5 min at 20°C). The supernatant was removed and the pellet resuspended in 100 μL ELISA sample buffer by repeated passage through a 0.5-mm-wide syringe needle. The suspension was transferred to an ELISA microtiter well precoated with MAb 58/0, and PVA detection was performed as above.

Protein–Protein Interactions Studied by the Yeast Two-Hybrid System

The VPg coding sequences were amplified from the infectious cDNA clones of wtPVA, PVA-a, and PVA-b3 or from the plasmid pRT-GFP-NIa (b) using appropriate primers containing the restriction sites needed for

cloning. The fibrillarin genes (open reading frames) Nb *Fib2a* and Nb *Fib2b* were amplified by PCR from cDNA synthesized from total RNA extracted from leaves of *N. benthamiana* using primers designed based on the published sequence (Kim et al., 2007b). The amplification products were sequenced and cloned in-frame with the GAL4 DNA binding domain (BD) and activation domain (AD) in the vectors pGBKT7 and pGADT7, respectively (Matchmaker Gal4 Yeast Two-Hybrid System 3; Clontech) and verified by sequencing. *Saccharomyces cerevisiae* (strain AH109) was cotransformed with the BD and AD plasmids using the lithium acetate method (Schiestl and Gietz, 1989). Protein–protein interactions were assessed at 30°C on a high-stringency selective medium lacking Trp, Leu, His, and adenine. The interaction between the *Simian virus 40* large T-antigen and the murine p53 protein expressed from plasmids pGADT7-T and pGBKT7-53, respectively (provided by Clontech), was used as a positive control, whereas the empty pGADT7 and pGBKT7 vectors (no insert) were used as negative controls.

Expression of the fusion proteins was assessed by growing transformed yeast strains in 5 mL of SD medium (Clontech) without Trp and Leu at 30°C overnight and isolating total proteins essentially as described (Volland et al., 1994). The protein pellet was dissolved in 100 μL of 2× Laemmli buffer (Laemmli, 1970) and boiled for 5 min. Proteins were analyzed by electrophoresis in a 12% SDS-polyacrylamide gel and electroblotted to a Hybond-P polyvinylidene difluoride membrane (Amersham). The membranes were probed with monoclonal antibodies (diluted 1:25,000) specific to the GAL4 DB and AD (Clontech). Signals were detected using horseradish peroxidase–conjugated secondary antibodies (Amersham Biosciences) (dilution 1:150,000) and the Super Signal West Pico chemiluminescent substrate system (Pierce).

Cosuppression Assays

For cosuppression assays, the VPg coding sequences were amplified by PCR from the infectious cDNA clones of wtPVA, PVA-a, PVA-b1, PVA-b2, PVA-b3, and PVA-b4 using appropriate primers including an AUG-start codon and an TAA-stop codon for VPg (see Supplemental Table 1 online). PCR products were cloned under the control of the 35S promoter fused to the PVA 5′-untranslated region in the binary pKOH200 vector as described (Savenkov and Valkonen, 2001). The resultant plasmids were named pA-VPg, pA-VPg(a), pA-VPg-b1, pA-VPg-b2, pA-VPg-b3, and pA-VPg-b4. Other pKOH200-based binary vectors contained the *UidA* (GUS) gene carrying a plant intron to prevent GUS expression in *A. tumefaciens* (Vancanneyt et al., 1990) (pA-GUS), the helper component proteinase (HC-Pro) coding sequence of PVA (Savenkov and Valkonen, 2001) (pA-HCpro), and the gene *mgfp4* (pBIN35S-GFP). These constructs have been described (Kreuze et al., 2005).

Binary vectors were electroporated into *A. tumefaciens* strain C58C1 with Ti plasmid pGV3850 as described above. Agroinfiltration (Johansen and Carrington, 2001) was performed using different *A. tumefaciens* cultures that were diluted with induction medium (10 mM $MgCl_2$ and 150 μM acetosyringone) to a final optical density of OD_{600} = 0.5. The cultures of the strain carrying pBIN35S-GFP and the strains carrying the other constructs were combined in a 1:3 ratio and used to infiltrate leaves of *N. benthamiana* line 16c.

Total RNA was extracted with TRIzol (Invitrogen) according to the manufacturer's instructions, and low and high molecular weight RNA fractions were separated as described (Kreuze et al., 2005). High molecular weight RNA (5 μg) was separated by formaldehyde gel electrophoresis, transferred to a Hybond-NX or Hybond-N membrane (Amersham Biosciences), fixed by UV light, and prehybridized and hybridized at 55°C overnight. The membrane was washed three times with 5× SSC (sodium chloride-sodium citrate buffer) + 0.5% SDS. For siRNA analysis, low molecular weight RNA (20 μg) was separated in a 15% PAGE gel containing 8 M urea. siRNA detection was performed as described (Pall and Hamilton, 2008). An antisense [α-^{32}P]UTP-labeled *gfp*-specific RNA probe was synthesized and used to detect *gfp* mRNA and siRNA as described (Kreuze et al., 2005).

BiFC

The VPg coding sequences and the fibrillarin genes Nb *Fib2a* and Nb *Fib2b* were amplified by PCR using appropriate primers containing restriction sites needed for cloning, and the products were cloned into the binary expression cassettes described by Zamyatnin et al. (2006). The VPg coding sequences and mutants were cloned in frame with the N-proximal or C-proximal half of the *yfp* gene to express the two halves of YFP (YN and YC, respectively) as a C-terminal fusion with VPg. The fibrillarin genes were cloned to express YN or YC fused to the N or C terminus of fibrillarin. All constructs were verified by sequencing. Binary vectors were electroporated into *A. tumefaciens* strain C58C1 cells containing the Ti plasmid pGV2260 as described above. The cultures of *A. tumefaciens* were resuspended in the induction media (10 mM $MgCl_2$ and 20 μM acetosyringone) at OD_{600} = 0.5, combined in a ratio of 1:1 (v/v), and agroinfiltrated into leaves of *N. benthamiana* as described above.

Analysis of Fibrillarin Silencing by Real-Time PCR

Total RNA was extracted with TRIzol (Invitrogen) according to manufacturer's instructions and treated with RQ1 RNase-free DNase (Promega) at 37°C for 30 min. The enzyme was then inactivated at 65°C for 10 min. cDNA synthesis was performed using *Moloney murine leukemia virus* reverse transcriptase (Promega) and random hexamers [$(dN)_6$] according to the manufacturer's instructions. Quantitative real-time PCR was performed with primers 5′-CAGAAGTGGAAGGGACTTGG-3′ and 5′-GGTGCCTAGCATCCTCAATAA-3′ designed by ProbeFinder software (Roche) according to the Nb *Fib2a* sequence excluding the N-terminal-most 441 bp used in the pTV-Fib2 vector. The primers were designed to amplify both Nb *Fib2a* and Nb *Fib2b*. Actin expression in *N. benthamiana* was assayed as an internal standard using primers 5′-GAGATTCCGCTGCCCAGAA-3′ and 5′-GAATGCCAGCAGCTTCCATT-3′. The LightCycler 480 SYBR Green I PCR Master Mix (Roche) and LightCycler 480 System (Roche) were used for the analysis. PCR amplification efficiency and relative gene expression were calculated by setting the threshold with the 2nd Derivative Maximum and calculating fold changes with the E-method ($E = E_T^{\,CpT(C)-CpT(S)} \times E_R^{\,CpR(S)-CpR(C)}$), where E_T is the efficiency of target, E_R is the efficiency of reference, CpT(C) is the Cp of the target (control), CpT(S) is the Cp of the target (sample), CpR(C) is the Cp of the reference (control), and CpR(S) is the Cp of the reference (sample), using LightCycler 480 Software (release 1.5.0 sp1).

Accession Numbers

Sequence data from this article can be found in the GenBank/EMBL databases under accession numbers FM244835 (Nb *Fib2b*), AM269909 (Nb *Fib2a*), and AJ296311 (full-length infectious cDNA clone of PVA-B11).

Supplemental Data

The following materials are available in the online version of this article.

Supplemental Figure 1. Protein Gel Blot Analysis and Subcellular Localization of GFP-NIa Fusion Proteins Expressed in Leaves of *Nicotiana benthamiana*.

Supplemental Figure 2. Subcellular Localization of VPg-GUS-GFP, PVAnls-GUS-GFP, and TEVnls-GUS-GFP Fusion Proteins as Observed by Epifluorescence Microscopy 3 DAI.

Supplemental Figure 3. Subnuclear Localization of GFP-NIa and GFP-VPg Fusion Proteins Expressed in Leaves of *Nicotiana benthamiana*.

Supplemental Figure 4. Visualization by Green Fluorescence of the Interaction between *Potato virus A* VPg and Fibrillarin in Nucleoli and Cajal Bodies Using a BiFC Assay.

Supplemental Figure 5. Virus-Induced Gene Silencing of Fibrillarin and Phytoene Desaturase in *Nicotiana benthamiana* using *Tobacco rattle virus* as a Vector.

Supplemental Figure 6. Expression of Fibrillarin mRNA in the Leaves of TRV-Fib2–Infected Plants Compared with the Leaves of TRV-Infected Plants.

Supplemental Figure 7. Multiple Sequence Alignment of the 60 N-Proximal Amino Acid Residues of VPg from 56 Potyviruses Shows That the NLS Regions Are Conserved in Genus *Potyvirus*.

Supplemental Table 1. Primers Used for Cloning or Site-Directed Mutagenesis.

ACKNOWLEDGMENTS

We thank Anna Germundsson for providing seeds of the VPg-transgenic *N. benthamiana* lines and participating in preliminary plant experiments, Sidona Sigorskaite for technical assistance, and Michael Taliansky for providing the AtFib2-mRFP and AtU2B″-mRFP clones. Financial support from the Academy of Finland (Grants 204104, 1102003, and 1118766) is gratefully acknowledged.

Received October 31, 2008; revised July 15, 2009; accepted July 31, 2009; published August 21, 2009.

REFERENCES

Anindya, R., Chittori, S., and Savithri, H.S. (2005). Tyrosine 66 of *Pepper vein banding virus* genome-linked protein is uridylylated by RNA-dependent RNA polymerase. Virology **336:** 154–162.

Anindya, R., and Savithri, H.S. (2004). Potyviral NIa proteinase, a proteinase with novel deoxyribonuclease activity. J. Biol. Chem. **279:** 32159–32169.

Banerjee, R., Weidman, M.K., Navarro, S., Comai, L., and Dasgupta, A. (2005). Modifications of both selectivity factor and upstream binding factor contribute to poliovirus-mediated inhibition of RNA polymerase I transcription. J. Gen. Virol. **86:** 2315–2322.

Beauchemin, C., Boutet, N., and Laliberté, J.-F. (2007). Visualization of the interaction between the precursors of VPg, the viral protein linked to the genome of *Turnip mosaic virus*, and the translation eukaryotic initiation factor iso 4E in planta. J. Virol. **81:** 775–782.

Beauchemin, C., and Laliberté, J.-F. (2007). The poly(A) binding protein is internalized in virus-induced vesicles or redistributed to the nucleolus during Turnip mosaic virus infection. J. Virol. **81:** 10905–10913.

Beven, A.F., Simpson, G.G., Brown, J.W.S., and Shaw, P.J. (1995). The organization of spliceosomal components in the nuclei of higher plants. J. Cell Sci. **108:** 509–518.

Boisvert, F.-M., van Koningsbruggen, S., Navascues, J., and Lamond, A.I. (2007). The multifunctional nucleolus. Nat. Rev. Mol. Cell Biol. **8:** 574–585.

Bortolamiol, D., Pazhouhandeh, M., Marrocco, K., Genschik, P., and Ziegler-Graff, V. (2007). The polerovirus F box protein P0 targets ARGONAUTE1 to suppress RNA silencing. Curr. Biol. **17:** 1615–1621.

Brigneti, G., Voinnet, O., Li, W.X., Ji, L.H., Ding, S.W., and Baulcombe, D.C. (1998). Viral pathogenicity determinants are suppressors of transgene silencing in *Nicotiana benthamiana.* EMBO J. **17:** 6739–6746.

Brosnan, C.A., Mitter, N., Christie, M., Smith, N.A., Waterhouse, P.M., and Carroll, B.J. (2007). Nuclear gene silencing directs reception of long-distance mRNA silencing in *Arabidopsis.* Proc. Natl. Acad. Sci. USA **104:** 14741–14746.

Canetta, E., Kim, S.H., Kalinina, N.O., Shaw, J., Adya, A.K., Gillespie, T., Brown, J.W.S., and Taliansky, M. (2008). A plant virus movement protein forms ringlike complexes with the major nucleolar protein, fibrillarin, *in vitro.* J. Mol. Biol. **376:** 932–937.

Canto, T., Uhrig, J.F., Swanson, M., Wright, K.M., and MacFarlane, S.A. (2006). Translocation of *Tomato bushy stunt virus* P19 protein into the nucleus by ALY proteins compromises its silencing suppressor activity. J. Virol. **80:** 9062–9072.

Carrington, J.C., and Dougherty, W.G. (1987). Small nuclear inclusion protein encoded by a plant potyvirus genome is a protease. J. Virol. **61:** 2540–2548.

Carrington, J.C., Freed, D.D., and Leinicke, A.J. (1991). Bipartite signal sequence mediates nuclear translocation of the plant potyviral NIa protein. Plant Cell **3:** 953–962.

Carrington, J.C., Haldeman, R., Dolja, V.V., and Restrepo-Hartwig, M.A. (1993). Internal cleavage and *trans*-proteolytic activities of the VPg-proteinase (NIa) of tobacco etch potyvirus in vivo. J. Virol. **67:** 6995–7000.

Chung, B.Y.-W., Miller, W.A., Atkins, J.F., and Firth, A.E. (2008). An overlapping essential gene in the Potyviridae. Proc. Natl. Acad. Sci. USA **105:** 5897–5902.

Denecke, J., and Vitale, A. (1995). The use of protoplasts to study protein synthesis and transport by the plant endomembrane system. Methods Cell Biol. **50:** 335–348.

Díaz-Pendón, J.A., and Shou-Wei, D. (2008). Direct and indirect roles of viral suppressors of RNA silencing in pathogenesis. Annu. Rev. Phytopathol. **46:** 303–326.

Dougherty, W.G., and Hiebert, E. (1980). Translation of potyvirus RNA in a rabbit reticulocyte lysate: Identification of nuclear inclusion proteins as products of tobacco etch virus RNA translation and cylindrical inclusion protein as a product of the potyvirus genome. Virology **104:** 174–182.

Dunoyer, P., Thomas, C., Harrison, S., Revers, F., and Maule, A. (2004). A cysteine-rich plant protein potentiates *Potyvirus* movement through an interaction with the virus genome-linked protein VPg. J. Virol. **78:** 2301–2309.

Edwardson, J.R., and Christie, R.G. (1983). Cytoplasmic cylindrical and nucleolar inclusions induced by potato virus-A. Phytopathology **73:** 290–293.

Gall, J.G. (2003). The centennial of the Cajal body. Nat. Rev. Mol. Cell Biol. **4:** 975–980.

Germundsson, A., Savenkov, E.I., Ala-Poikela, M., and Valkonen, J.P.T. (2007). VPg of *Potato virus A* alone does not suppress RNA silencing but affects virulence of a heterologous virus. Virus Genes **34:** 387–399.

Germundsson, A., and Valkonen, J.P.T. (2006). P1- and VPg-transgenic plants show similar resistance to *Potato virus A* and may compromise long distance movement of the virus in plant sections expressing RNA silencing-based resistance. Virus Res. **116:** 208–213.

Goldbach, R. (1986). Molecular evolution of plant RNA viruses. Annu. Rev. Phytopathol. **24:** 289–310.

Grebenok, R.J., Pierson, E., Lambert, G.M., Gong, F.-C., Afonso, C.L., Haldeman-Cahill, R., Carrington, J.C., and Galbraith, D.W. (1997). Green-fluorescent protein fusions for efficient characterization of nuclear targeting. Plant J. **11:** 573–586.

Grzela, R., Szolajska, E., Ebel, C., Madern, D., Favier, A., Wojtal, I., Zagorski, W., and Chroboczek, J. (2008). Virulence factor of potato virus Y, genome-attached terminal protein VPg, is a highly disordered protein. J. Biol. Chem. **283:** 213–221.

Guo, D., Rajamäki, M.-L., Saarma, M., and Valkonen, J.P.T. (2001).

Towards a protein interaction map of potyviruses: Protein interaction matrixes of two potyviruses based on the yeast two-hybrid system. J. Gen. Virol. **82:** 935–939.

Haas, G., Azevedo, J., Moissiard, G., Geldreich, A., Himber, C., Bureau, M., Fukuhara, T., Keller, M., and Voinnet, O. (2008). Nuclear import of CaMV P6 is required for infection and suppression of the RNA silencing factor DRB4. EMBO J. **27:** 2102–2112.

Hajimorad, M.R., Ding, X.S., Flasinski, S., Mahajan, S., Graff, E., Haldeman-Cahill, R., Carrington, J.C., and Cassidy, B.G. (1996). NIa and NIb of peanut stripe potyvirus are present in the nucleus of infected cells, but do not form inclusions. Virology **224:** 368–379.

Hiscox, J.A. (2003). The interaction of animal cytoplasmic RNA viruses with the nucleus to facilitate replication. Virus Res. **95:** 13–22.

Hiscox, J.A. (2007). RNA viruses: Hijacking the dynamic nucleolus. Nat. Rev. Microbiol. **5:** 119–127.

Hong, Y., Levay, K., Murphy, J.F., Klein, P.G., Shaw, J.G., and Hunt, A.G. (1995). A potyvirus polymerase interacts with the viral coat protein and VPg in yeast cells. Virology **214:** 159–166.

Hämäläinen, J.H., Kekarainen, T., Gebhardt, C., Watanabe, K.N., and Valkonen, J.P.T. (2000). Recessive and dominant genes interfere with the vascular transport of Potato virus A in diploid potatoes. Mol. Plant Microbe Interact. **13:** 402–412.

Izumi, R.E., Valdez, B., Banerjee, R., Srivastava, M., and Dasgupta, A. (2001). Nucleolin stimulates viral internal ribosome entry site-mediated translation. Virus Res. **76:** 17–29.

Johansen, L.K., and Carrington, J.C. (2001). Silencing on the spot. Induction and suppression of RNA silencing in the *Agrobacterium*-mediated transient expression system. Plant Physiol. **126:** 930–938.

Keller, K.E., Johansen, I.E., Martin, R.R., and Hampton, R.O. (1998). Potyvirus genome-linked protein (VPg) determines pea seed-borne mosaic virus pathotype-specific virulence in *Pisum sativum.* Mol. Plant Microbe Interact. **11:** 124–130.

Kim, S.H., MacFarlane, S., Kalinina, N.O., Rakitina, D.V., Ryabov, E.V., Gillespie, T., Haupt, S., Brown, J.W.S., and Taliansky, M. (2007a). Interaction of a plant virus-encoded protein with the major nucleolar protein fibrillarin is required for systemic virus infection. Proc. Natl. Acad. Sci. USA **104:** 11115–11120.

Kim, S.H., Ryabov, E.V., Kalinina, N.O., Rakitina, D.V., Gillespie, T., MacFarlane, S., Haupt, S., Brown, J.W.S., and Taliansky, M. (2007b). Cajal bodies and the nucleolus are required for a plant virus systemic infection. EMBO J. **26:** 2169–2179.

Knuhtsen, H., Hiebert, E., and Purcifull, D.E. (1974). Partial purification and some properties of tobacco etch virus induced intranuclear inclusions. Virology **61:** 200–209.

Kreuze, J.F., Savenkov, E.I., Cuellar, W., Li, X., and Valkonen, J.P.T. (2005). Viral class 1 RNase III involved in suppression of RNA silencing. J. Virol. **79:** 7227–7238.

Laemmli, U.K. (1970). Cleavage of structural proteins during the assembly of the head of bacteriophage T4. Nature **227:** 680–685.

Léonard, S., Plante, D., Wittmann, S., Daigneault, N., Fortin, M.G., and Laliberté, J.-F. (2000). Complex formation between potyvirus VPg and translation eukaryotic initiation factor 4E correlates with virus infectivity. J. Virol. **74:** 7730–7737.

Léonard, S., Viel, C., Beauchemin, C., Daigneault, N., Fortin, M.G., and Laliberté, J.-F. (2004). Interaction of VPg-Pro of *Turnip mosaic virus* with the translation initiation factor 4E and the poly(A)-binding protein *in planta.* J. Gen. Virol. **85:** 1055–1063.

Li, X.H., Valdez, P., Olvera, R.E., and Carrington, J.C. (1997). Functions of the tobacco etch virus RNA polymerase (NIb): Subcellular transport and protein-protein interaction with VPg/Proteinase (NIa). J. Virol. **71:** 1598–1607.

Llave, C., Kasschau, K.D., and Carrington, J.C. (2000). Virus-encoded suppressor of posttranscriptional gene silencing targets a maintenance step in the silencing pathway. Proc. Natl. Acad. Sci. USA **97:** 13401–13406.

Lucy, A.P., Guo, H.S., Li, W.X., and Ding, S.W. (2000). Suppression of post-transcriptional gene silencing by a plant viral protein localized in the nucleus. EMBO J. **19:** 1672–1680.

Martin, M.T., Garcia, J.A., Cervera, M.T., Goldbach, R.W., and van Lent, J.W.M. (1992). Intracellular localization of three non-structural plum pox potyvirus proteins by immunogold labelling. Virus Res. **25:** 201–211.

Miller, S., and Krijinse-Locker, J. (2008). Modification of intracellular membrane structures for virus replication. Nat. Rev. Microbiol. **6:** 363–374.

Morozov, S.Yu., Fedorkin, O.N., Jüttner, G., Schiemann, J., Baulcombe, D.C., and Atabekov, J.G. (1997). Complementation of a potato virus X mutant mediated by bombardment of plant tissues with cloned virus movement protein genes. J. Gen. Virol. **78:** 2077–2083.

Murphy, J.F., Klein, P.G., Hunt, A.G., and Shaw, J.G. (1996). Replacement of the tyrosine residue that links a potyviral VPg to the viral RNA is lethal. Virology **220:** 535–538.

Murphy, J.F., Rychlik, W., Rhoads, R.E., Hunt, A.G., and Shaw, J.G. (1991). A tyrosine residue in the small nuclear inclusion protein of tobacco vein mottling virus links the VPg to the viral RNA. J. Virol. **65:** 511–513.

Nicolas, O., Dunnington, S.W., Gotow, L.F., Pirone, T.P., and Hellmann, G.M. (1997). Variations in the VPg protein allow a potyvirus to overcome *va* gene resistance in tobacco. Virology **237:** 452–459.

Olson, M.O.J., Dundr, M., and Szebeni, A. (2000). The nucleolus: An old factory with unexpected capabilities. Trends Cell Biol. **10:** 189–196.

Pall, G.S., and Hamilton, A.J. (2008). Improved northern blot method for enhanced detection of small RNA. Nat. Protoc. **3:** 1077–1084.

Pontes, O., Li, C.F., Nunes, P.C., Haag, J., Ream, T., Vitins, A., Jacobsen, S.E., and Pikaard, C.S. (2006). The *Arabidopsis* chromatin-modifying nuclear siRNA pathway involves a nucleolar RNA processing center. Cell **126:** 79–92.

Pontes, O., and Pikaard, C.S. (2008). siRNA and miRNA processing: New functions for Cajal bodies. Curr. Opin. Genet. Dev. **18:** 197–203.

Puurand, Ü., Valkonen, J.P.T., Mäkinen, K., Rabenstein, F., and Saarma, M. (1996). Infectious in vitro transcripts from cloned cDNA of the potato A potyvirus. Virus Res. **40:** 135–140.

Puustinen, P., and Mäkinen, K. (2004). Uridylylation of the potyvirus VPg by viral replicase NIb correlates with the nucleotide binding capacity of VPg. J. Biol. Chem. **279:** 38103–38110.

Rajamäki, M., Merits, A., Rabenstein, F., Andrejeva, J., Paulin, L., Kekarainen, T., Kreuze, J.F., Forster, R.L.S., and Valkonen, J.P.T. (1998). Biological, serological, and molecular differences among isolates of potato A potyvirus. Phytopathology **88:** 311–321.

Rajamäki, M.-L., Kelloniemi, J., Alminaite, A., Kekarainen, T., Rabenstein, F., and Valkonen, J.P.T. (2005). A novel insertion site inside the potyvirus P1 cistron allows expression of heterologous proteins and suggests some P1 functions. Virology **342:** 88–101.

Rajamäki, M.-L., Mäki-Valkama, T., Mäkinen, K., and Valkonen, J.P.T. (2004). Infection with potyviruses. In Plant-Pathogen Interactions. N. Talbot, ed (Oxford, UK: Blackwell Publishing), pp. 68–91.

Rajamäki, M.-L., and Valkonen, J.P.T. (1999). The 6K2 protein and the VPg of potato virus A are determinants of systemic infection in *Nicandra physaloides.* Mol. Plant Microbe Interact. **12:** 1074–1081.

Rajamäki, M.-L., and Valkonen, J.P.T. (2002). Viral genome-linked protein (VPg) controls accumulation and phloem-loading of a potyvirus in inoculated potato leaves. Mol. Plant Microbe Interact. **15:** 138–149.

Rajamäki, M.-L., and Valkonen, J.P.T. (2003). Localization of a potyvirus and the viral genome-linked protein in wild potato leaves at an early stage of systemic infection. Mol. Plant Microbe Interact. **16:** 25–34.

Rajamäki, M.-L., and Valkonen, J.P.T. (2004). Detection of a natural point mutation in *Potato virus A* that overcomes resistance to vascular movement in *Nicandra physaloides*, and studies on seed-transmissibility of the mutant virus. Ann. Appl. Biol. **144:** 77–86.

Rantalainen, K.I., Uversky, V.N., Permi, P., Kalkkinen, N., Dunker, A.K., and Mäkinen, K. (2008). Potato virus A genome-linked protein VPg is an intrinsically disordered molten globule-like protein with a hydrophobic core. Virology **377:** 280–288.

Ratcliff, F., Martin-Hernandez, A.M., and Baulcombe, D.C. (2001). Tobacco rattle virus as a vector for analysis of gene function by silencing. Plant J. **25:** 237–245.

Restrepo, M.A., Freed, D.D., and Carrington, J.C. (1990). Nuclear transport of plant potyviral proteins. Plant Cell **2:** 987–998.

Robaglia, C., and Caranta, C. (2006). Translation initiation factors: A weak link in plant RNA virus infection. Trends Plant Sci. **11:** 40–45.

Ruiz-Ferrer, V., and Voinnet, O. (2009). Roles of plant small RNAs in biotic stress responses. Annu. Rev. Plant Biol. **60:** 485–510.

Ryabov, E.F., Kim, S.H., and Taliansky, M. (2004). Identification of a nuclear localization signal and nuclear export signal of the umbraviral long-distance RNA movement protein. J. Gen. Virol. **85:** 1329–1333.

Salmenkallio-Marttila, M., Aspegren, K., Åkerman, S., Kurtén, U., Mannonen, L., Ritala, A., Teeri, T.H., and Kauppinen, V. (1995). Transgenic barley (*Hordeum vulgare* L.) by electroporation of protoplasts. Plant Cell Rep. **15:** 301–304.

Salonen, A., Ahola, T., and Kääriäinen, L. (2004). Viral RNA replication in association with cellular membranes. Curr. Top. Microbiol. Immunol. **285:** 139–173.

Sambrook, J., and Russell, D.W. (2001). Molecular Cloning: A Laboratory Manual. (Cold Spring Harbor, NY: Cold Spring Harbor Laboratory Press).

Savenkov, E.I., and Valkonen, J.P.T. (2001). Potyviral helper component-proteinase expressed in transgenic plants enhaces titers of *Potato leaf roll virus* but does not alleviate its phloem-limitation. Virology **283:** 285–293.

Schaad, M.C., Anderberg, R.J., and Carrington, J.C. (2000). Strain-specific interaction of the tobacco etch virus NIa protein with the translation initiation factor eIF4E in the yeast two-hybrid system. Virology **273:** 300–306.

Schaad, M.C., Haldeman-Cahill, R., Cronin, S., and Carrington, J.C. (1996). Analysis of the VPg-proteinase (NIa) encoded by tobacco etch potyvirus: Effects of mutations on subcellular transport, proteolytic processing, and genome amplification. J. Virol. **70:** 7039–7048.

Schaad, M.C., Lellis, A.D., and Carrington, J.C. (1997). VPg of tobacco etch potyvirus is a host genotype-specific determinant for long-distance movement. J. Virol. **71:** 8624–8631.

Schiestl, R.H., and Gietz, R.D. (1989). High efficiency transformation of intact yeast cells using single-stranded nucleic acids as a carrier. Curr. Genet. **16:** 339–346.

Solovyev, A.G., Stroganova, T.A., Zamyatnin, A.A., Jr., Fedorkin, O.N., Schiemann, J., and Morozov, S.Yu. (2000). Subcellular sorting of small membrane-associated triple gene block proteins: TGBp3-assisted targeting of TGBp2. Virology **269:** 113–127.

Thivierge, K., Cotton, S., Dufresne, P.J., Mathieu, I., Beauchemin, C., Ide, C., Fortin, M.G., and Laliberte, J.-F. (2008). Eukaryotic elongation factor 1A interacts with *Turnip mosaic virus* RNA-dependent RNA polymerase and VPg-Pro in virus-induced vesicles. Virology **377:** 216–225.

Vancanneyt, G., Schmidt, R., O'Conner-Sanchez, A., Willmitzer, L., and Rocha-Sosa, M. (1990). Construction of an intron-containing marker gene: splicing of the intron in transgenic plants and its use in monitoring early events in *Agrobacterium*-mediated plant transformation. Mol. Gen. Genet. **220:** 245–250.

Volland, C., Urban-Grimal, D., Géraud, G., and Haguenauer-Tsapis, R. (1994). Endocytosis and degradation of the yeast uracil permease under adverse conditions. J. Biol. Chem. **269:** 9833–9841.

Waggoner, S., and Sarnow, P. (1998). Viral ribonucleoprotein complex formation and nucleolar-cytoplasmic relocalization of nucleolin in poliovirus-infected cells. J. Virol. **72:** 6699–6709.

Wang, D., and Maule, A.J. (1995). Inhibition of host gene expression associated with plant virus replication. Science **267:** 229–231.

Wittmann, S., Chatel, H., Fortin, M.G., and Laliberté, J.-F. (1997). Interaction of the viral protein genome linked of Turnip mosaic potyvirus with the translational eukaryotic initiation factor (iso) 4E of *Arabidopsis thaliana* using the yeast two-hybrid system. Virology **234:** 84–92.

Yang, S.-J., Carter, S.A., Cole, A.B., Cheng, N.-H., and Nelson, R.S. (2004). A natural variant of a host RNA-dependent RNA polymerase is associated with increase susceptibility to viruses in *N. benthamiana.* Proc. Natl. Acad. Sci. USA **101:** 6297–6302.

Zamyatnin, A.A., Jr., Solovyev, A.G., Bozhkov, P.V., Valkonen, J.P. T., Morozov, S.Y., and Savenkov, E.I. (2006). Assessment of the integral membrane protein topology in living cells. Plant J. **46:** 145–154.

Zamyatnin, A.A., Jr., Solovyev, A.G., Savenkov, E.I., Germundsson, A., Sandgren, M., Valkonen, J.P.T., and Morozov, S.Y. (2004). Transient coexpression of individual genes encoded by the triple gene block of *Potato mop-top virus* reveals requirements for TGBp1 trafficking. Mol. Plant Microbe Interact. **17:** 921–930.

Zhang, X., Yuan, Y.-R., Pei, Y., Lin, S.-S., Tuschl, T., Patel, D.J., and Chua, N.-H. (2006). *Cucumber mosaic virus*-encoded 2b suppressor inhibits *Arabidopsis* Argonaute1 cleavage activity to counter plant defense. Genes Dev. **20:** 3255–3268.